Electronic Supplementary Material (ESI) for RSC Advances.

Supporting Information

Highly Efficient Ru(II)-Alkylidene Based Hoveyda-Grubbs Catalysts for Ring-Closing Metathesis Reactions

Mariam Y. Al-Enezi, Elizabeth John, Yehia A. Ibrahim and Nouria A. Al-Awadi*

**Chemistry Department, Kuwait University, P.O. Box 5969, Safat 13060, Kuwait.*

Email: na.nabaq.kw@gmail.com

Table of Contents

NMR spectra

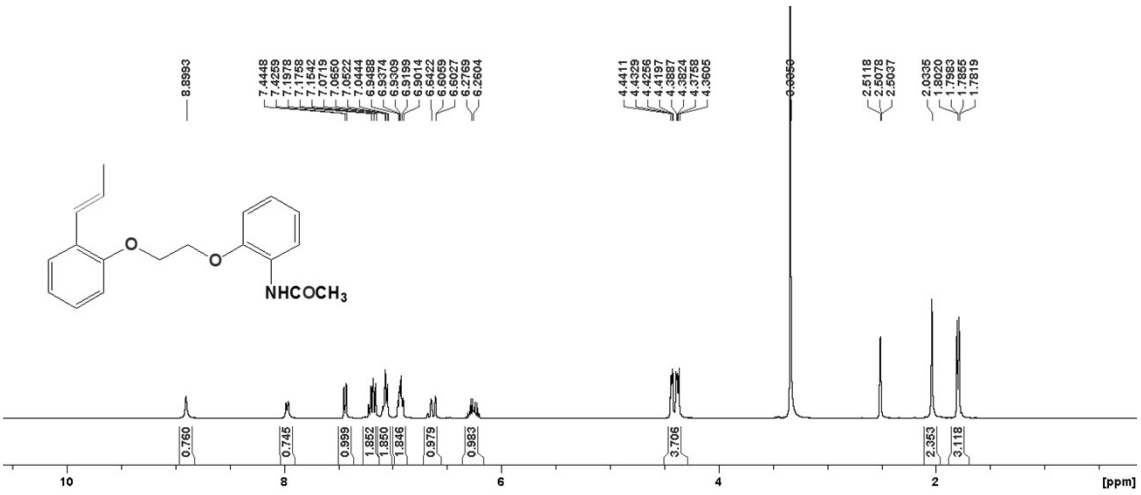

Figure S1. ^{1}H-NMR spectrum of **6a** in DMSO-d_6 at 25 ^{0}C.

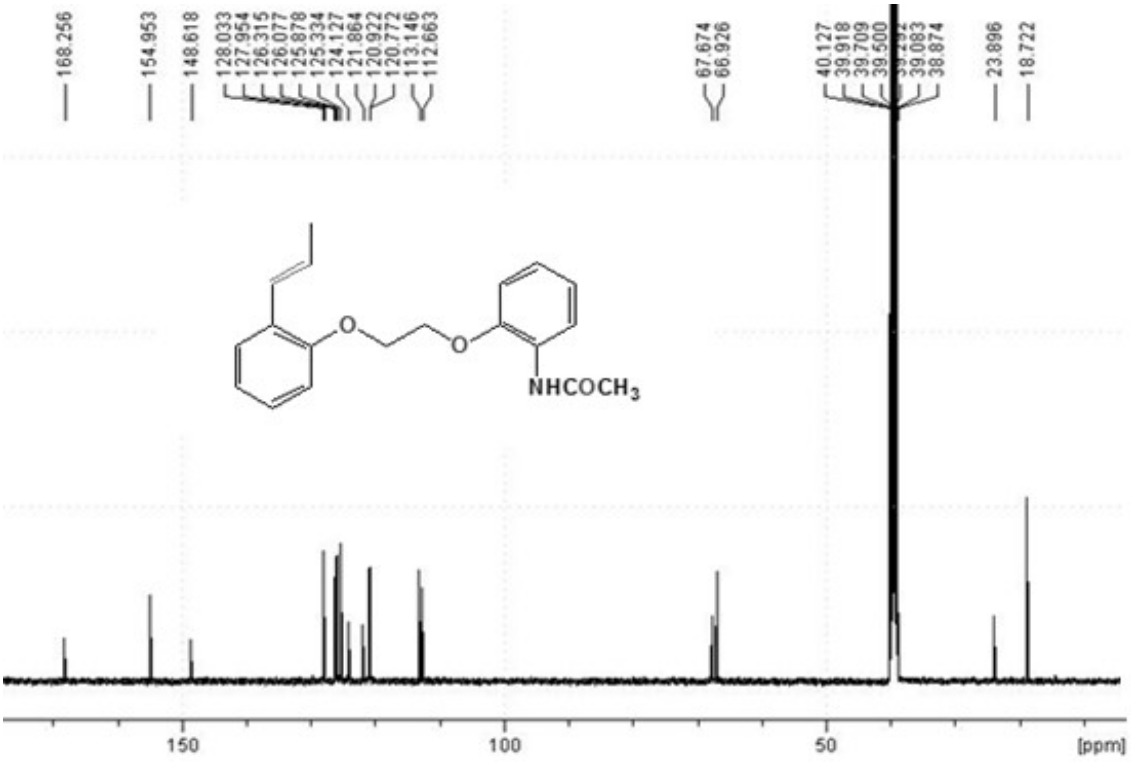

Figure S2. ^{13}C-NMR spectrum of **6a** in DMSO-d_6 at 25 ^{0}C.

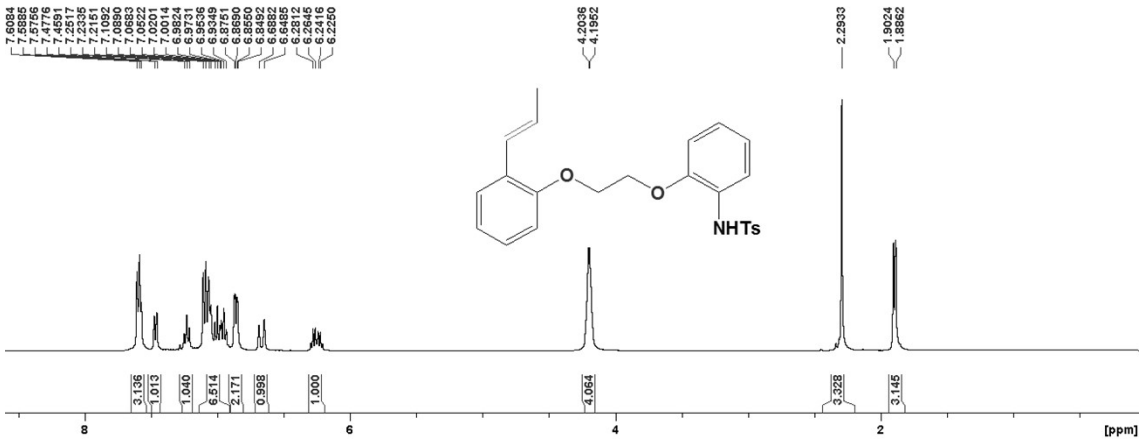

Figure S3. ^{1}H-NMR spectrum of **6b** in $CDCl_3$ at 25 ^{0}C.

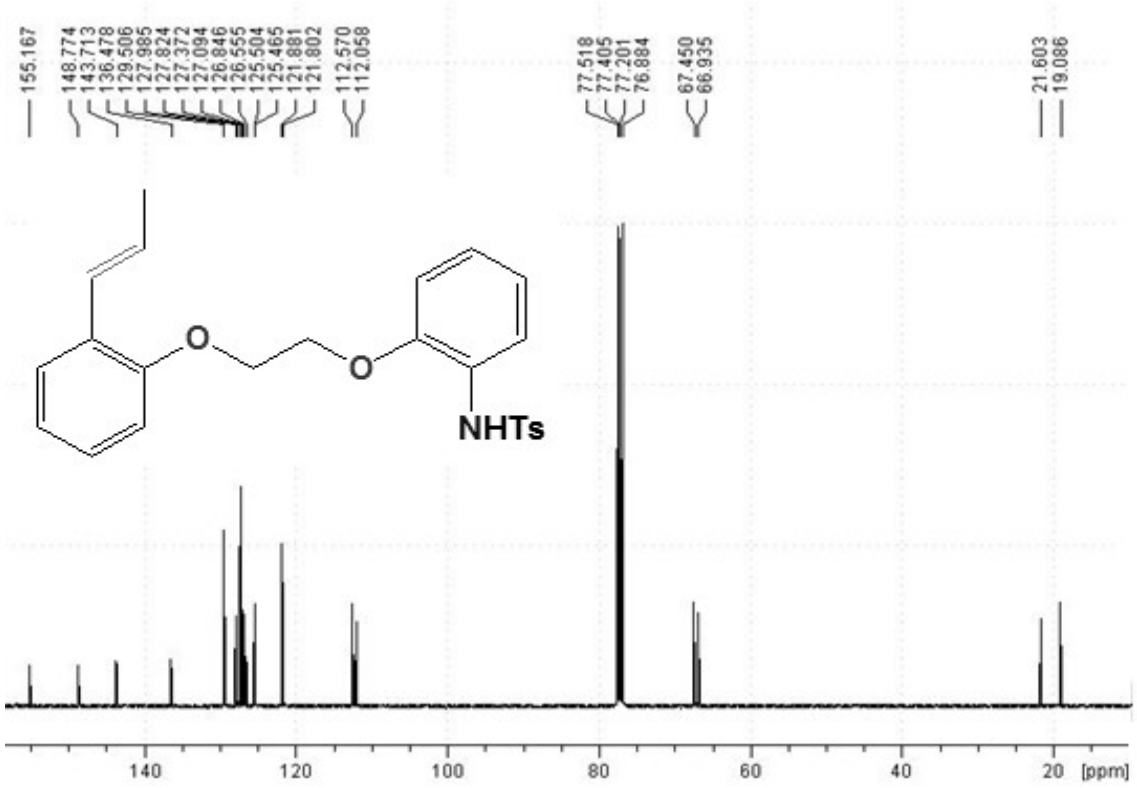

Figure S4. ^{13}C-NMR spectrum of **6b** in $CDCl_3$ at 25 ^{0}C.

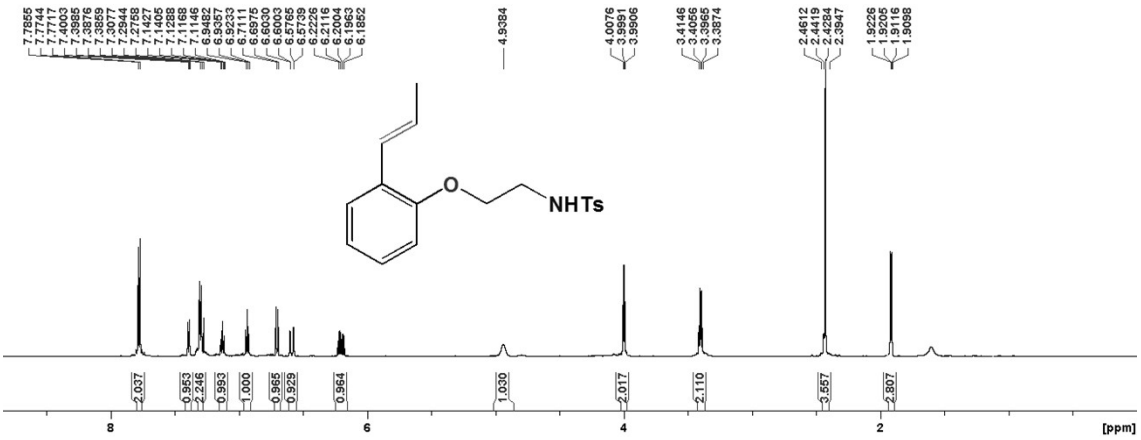

Figure S5. ^{1}H-NMR spectrum of **6c** in $CDCl_3$ at 25 ^{0}C.

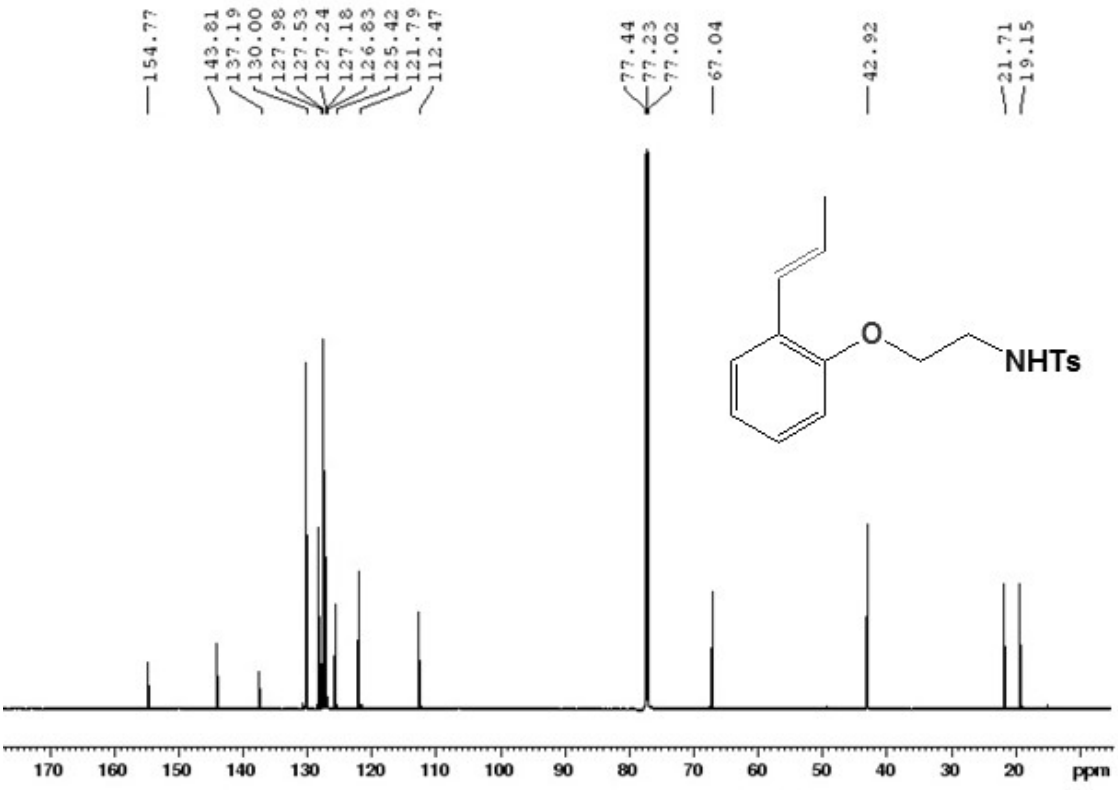

Figure S6. ^{13}C-NMR spectrum of **6c** in $CDCl_3$ at 25 ^{0}C.

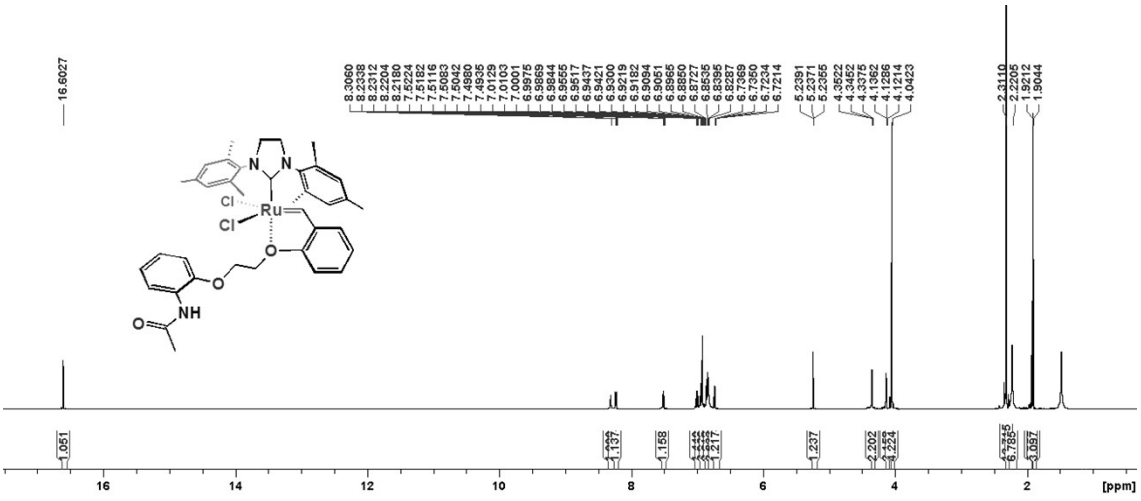

Figure S7. ^{1}H-NMR spectrum of **7a** in CD_2Cl_2 at 25 ^{0}C.

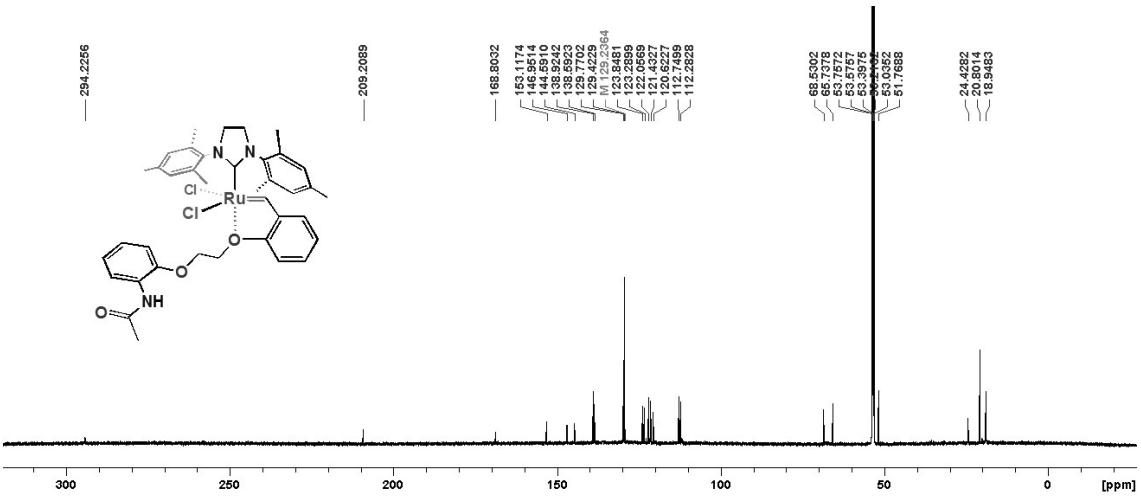

Figure S8. ^{13}C-NMR spectrum of **7a** in CD_2Cl_2 at 25 ^{0}C.

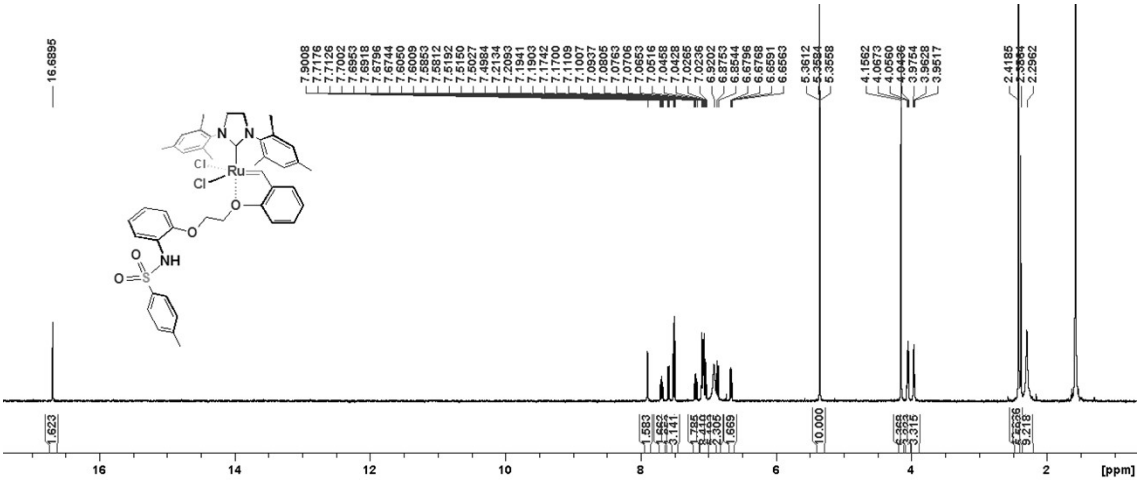

Figure S9. ^{1}H-NMR spectrum of **7b** in CD_2Cl_2 at 25 ^{0}C.

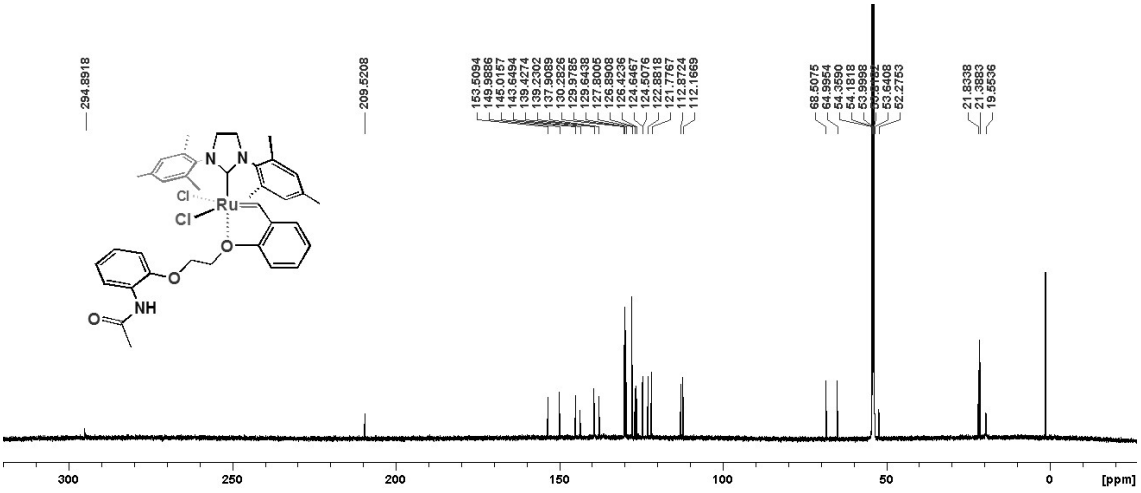

Figure S10. ^{13}C-NMR spectrum of **7b** in CD_2Cl_2 at 25 ^{0}C.

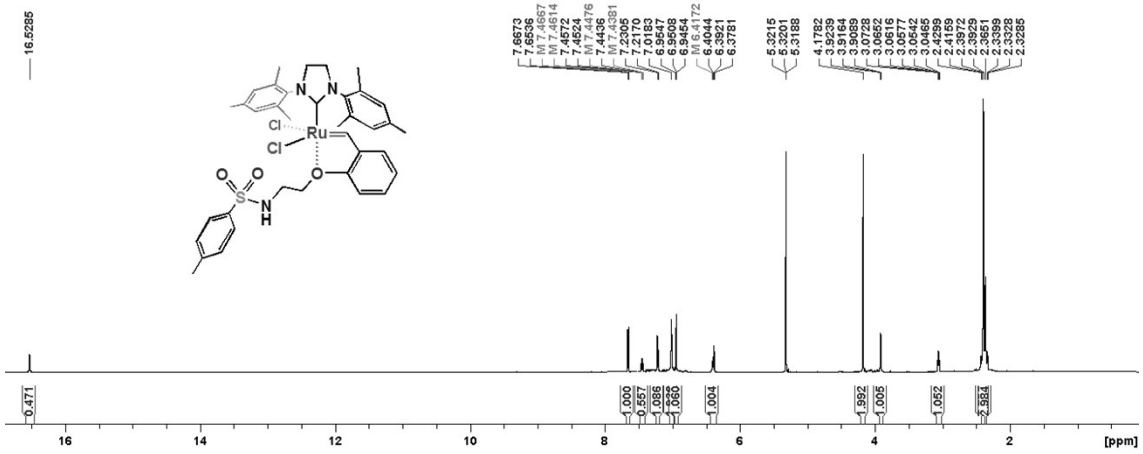

Figure S11. ^{1}H-NMR spectrum of **7c** in CD_2Cl_2 at 25 ^{0}C.

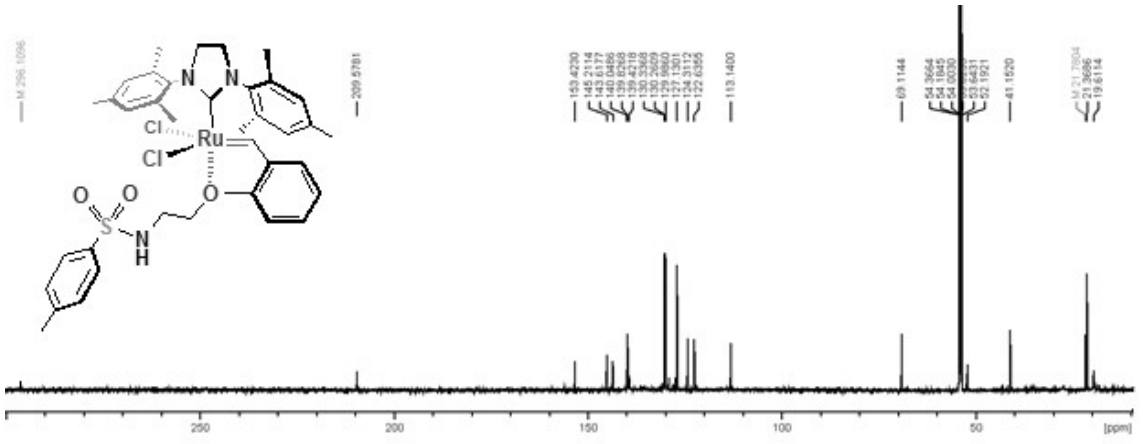

Figure S12. ^{13}C-NMR spectrum of **7c** in CD_2Cl_2 at 25 ^{0}C.

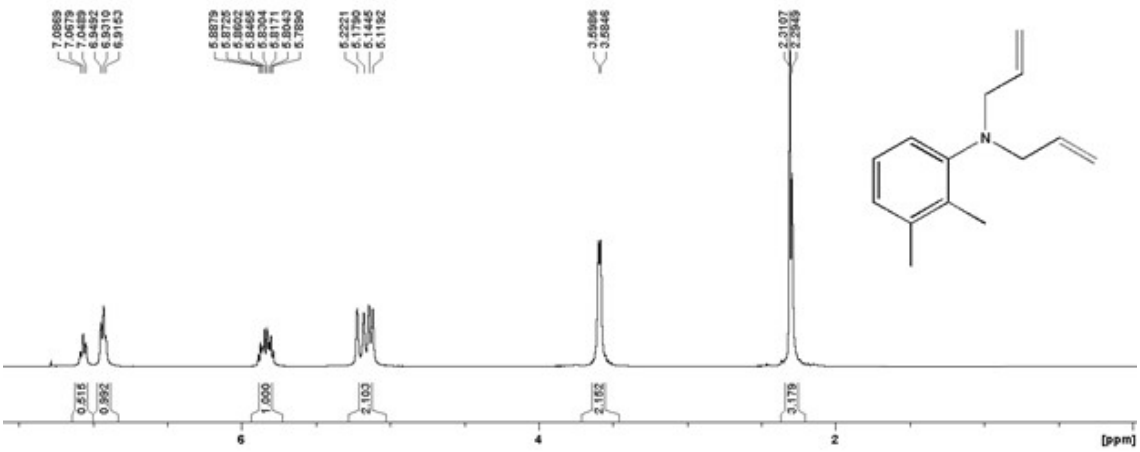

Figure S13. ^{1}H-NMR spectrum of **8i** in $CDCl_3$ at 25 ^{0}C.

Figure S14. ^{13}C-NMR spectrum of **8i** in $CDCl_3$ at 25 ^{0}C.

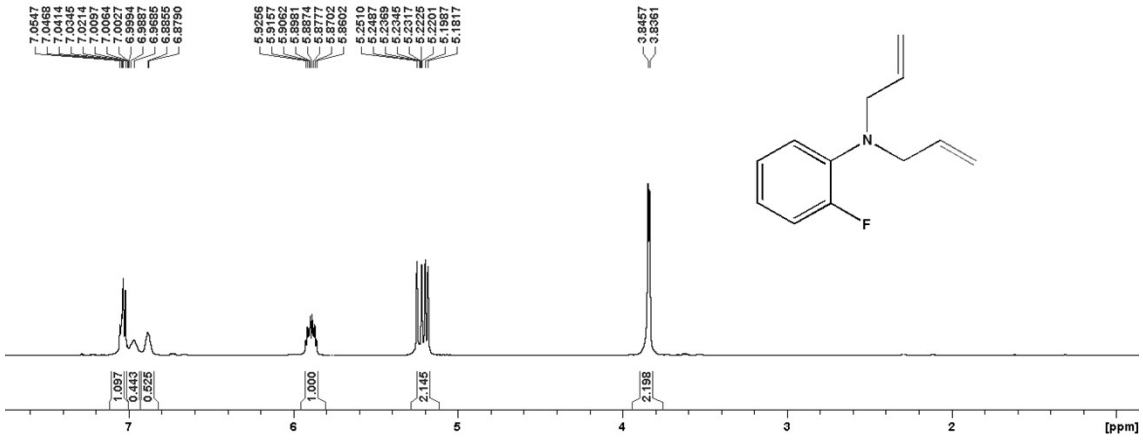

Figure S15. ^{1}H-NMR spectrum of **8k** in $CDCl_3$ at 25 ^{0}C.

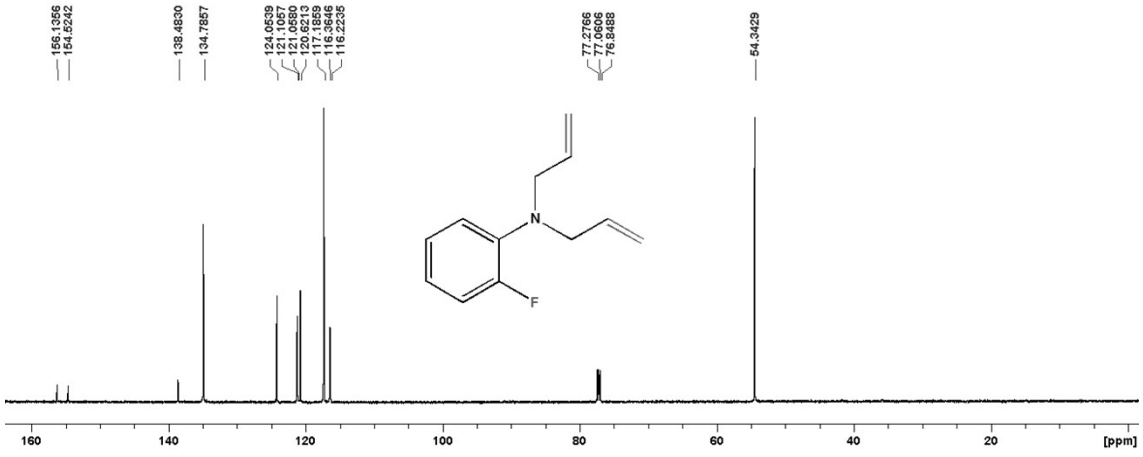

Figure S16. ^{13}C-NMR spectrum of **8k** in $CDCl_3$ at 25 ^{0}C.

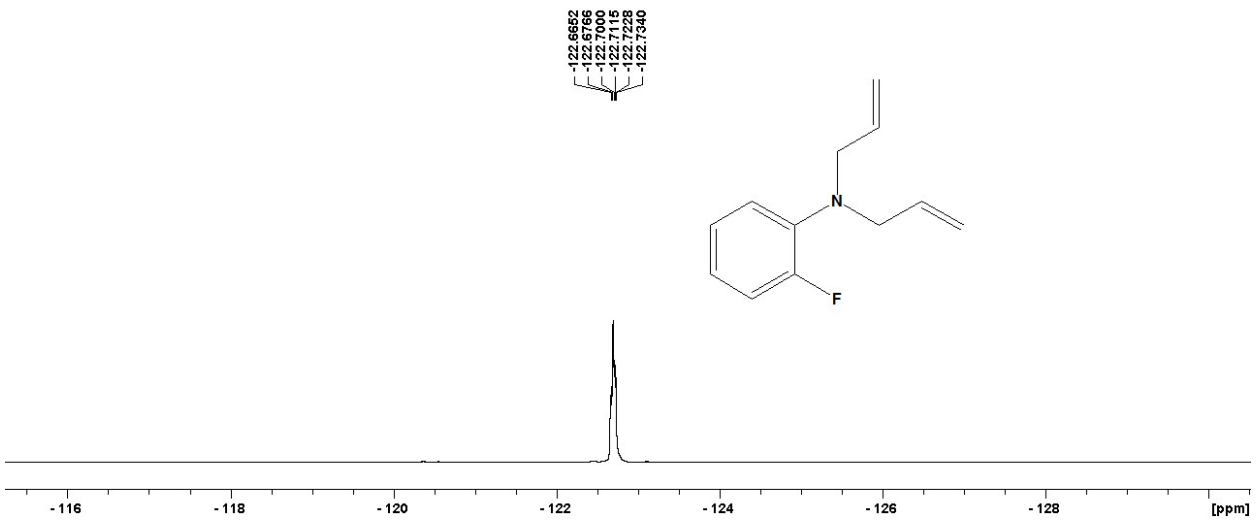

Figure S17. 19F NMR spectrum of **8k** in $CDCl_3$ at 25 ^{0}C.

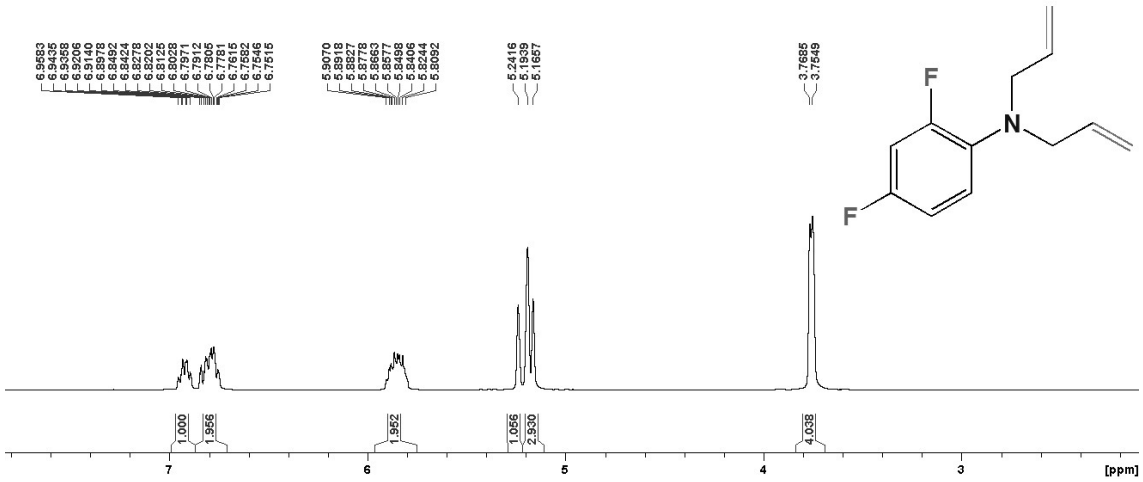

Figure S18. ^{1}H-NMR spectrum of **8o** in $CDCl_3$ at 25 ^{0}C.

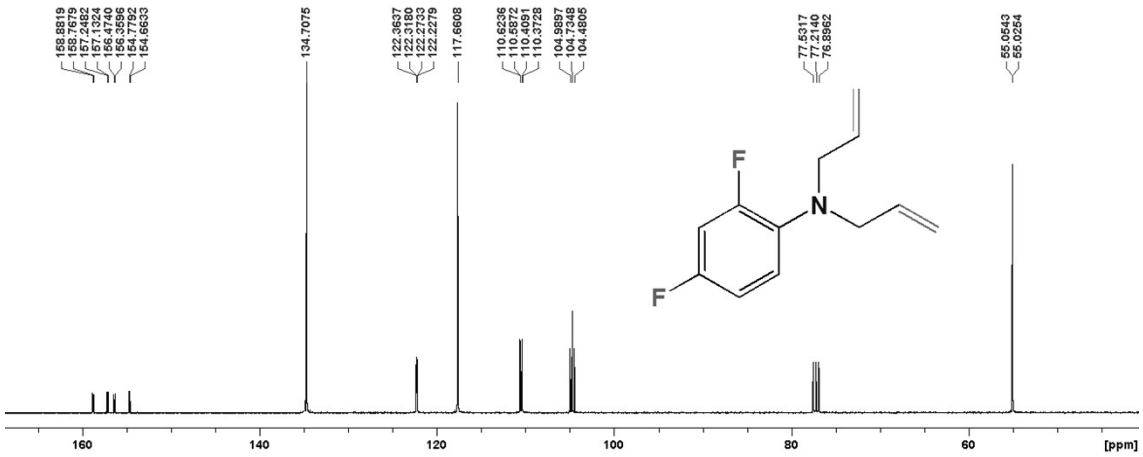

Figure S19. ^{13}C-NMR spectrum of **8o** in $CDCl_3$ at 25 ^{0}C.

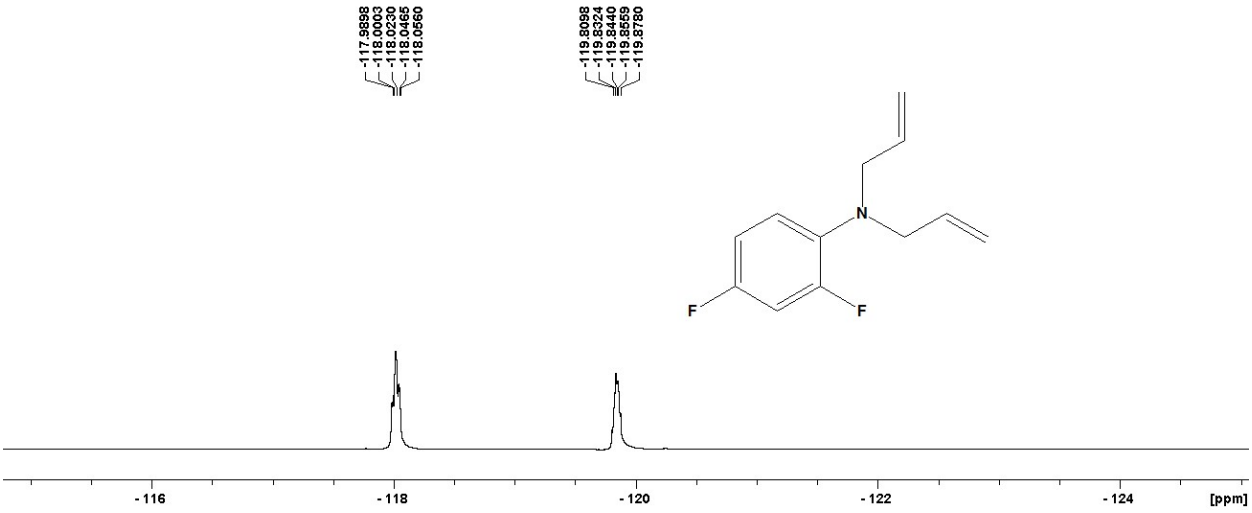

Figure S20. 19F NMR spectrum of **8o** in $CDCl_3$ at 25 ^{0}C.

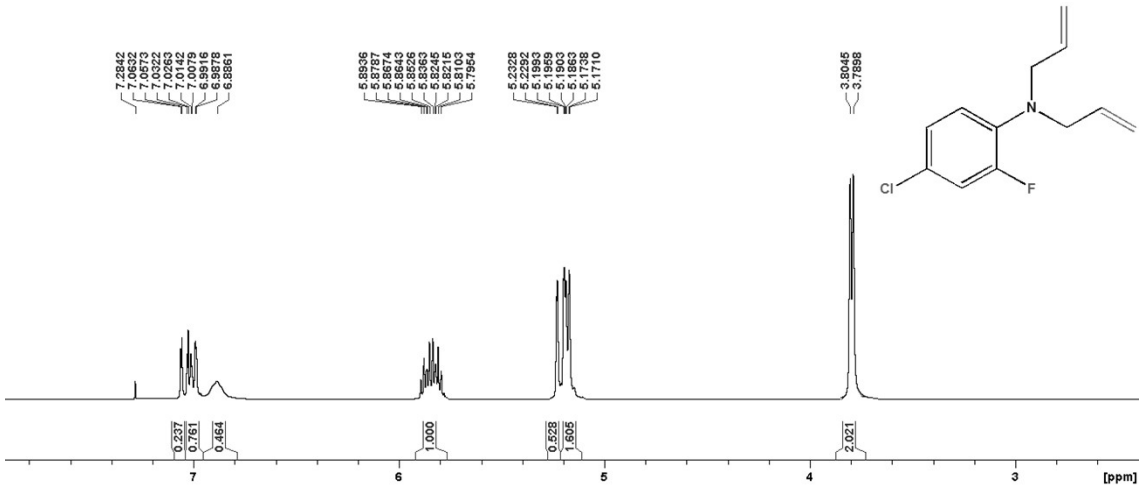

Figure S21. ^{1}H-NMR spectrum of **8q** in $CDCl_3$ at 25 ^{0}C.

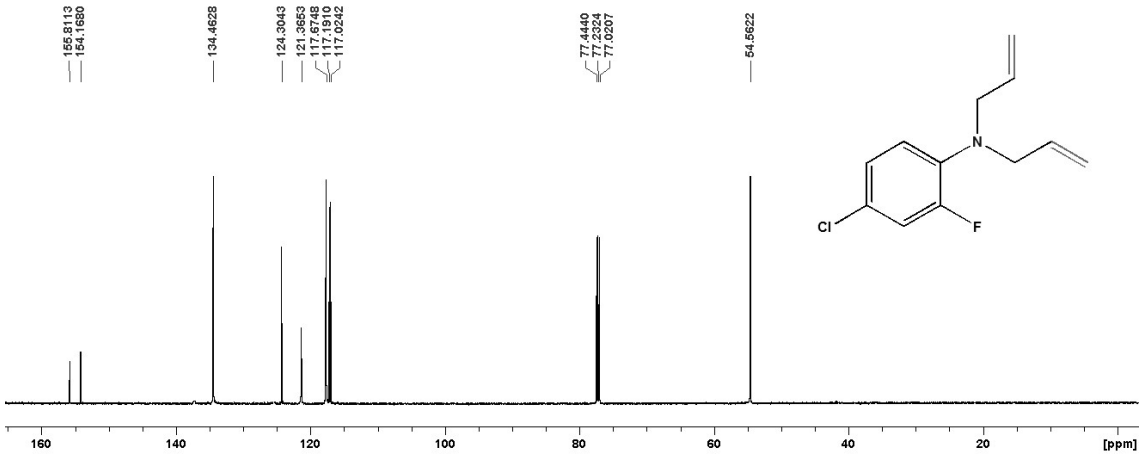

Figure S22. ^{13}C-NMR spectrum of **8q** in $CDCl_3$ at 25 ^{0}C.

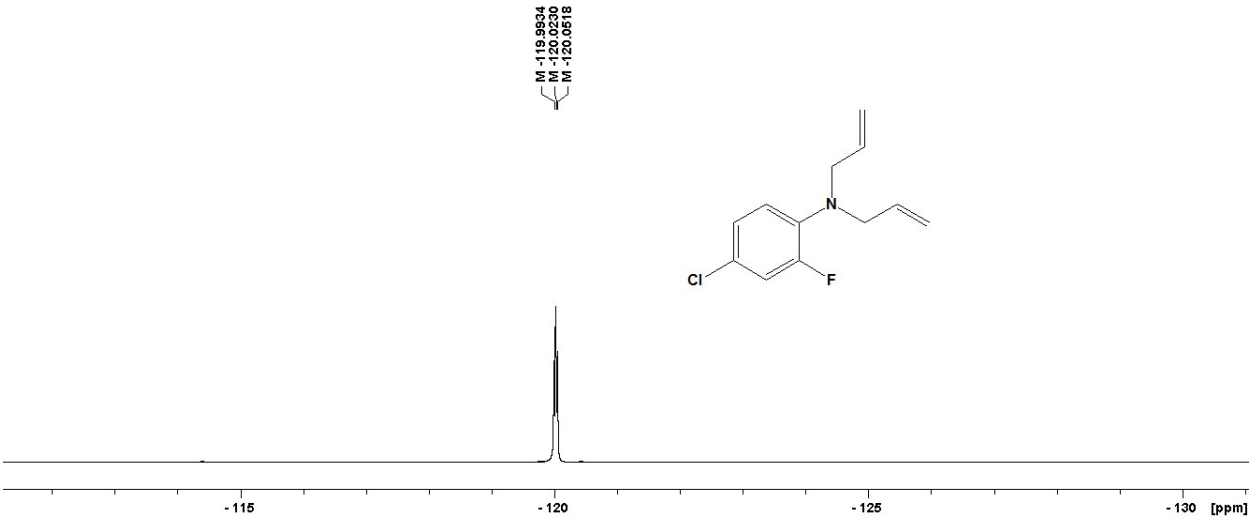

Figure S23. 19F NMR spectrum of **8q** in $CDCl_3$ at 25 ^{0}C.

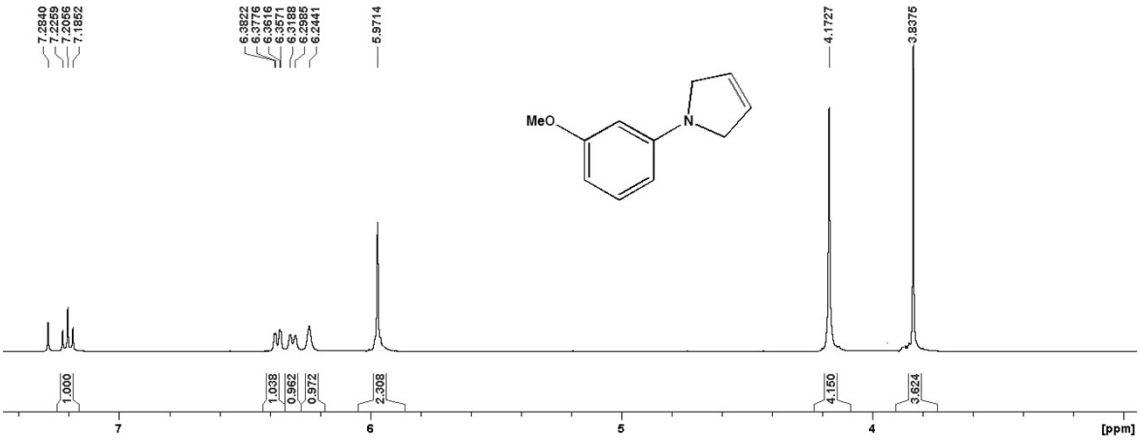

Figure S24. ^{1}H-NMR spectrum of **9f** in $CDCl_3$ at 25 ^{0}C.

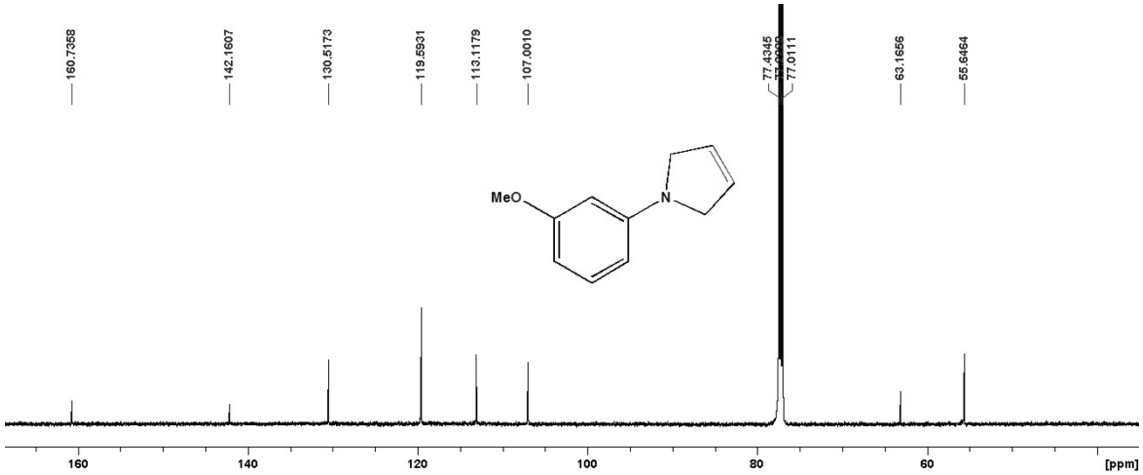

Figure S25. ^{13}C-NMR spectrum of **9f** in $CDCl_3$ at 25 ^{0}C.

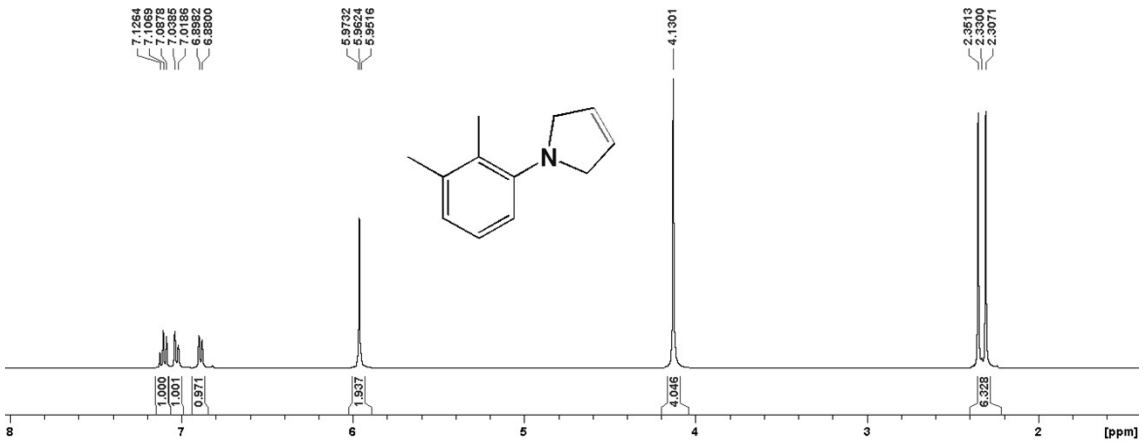

Figure S26. ^{1}H-NMR spectrum of **9i** in $CDCl_3$ at 25 ^{0}C.

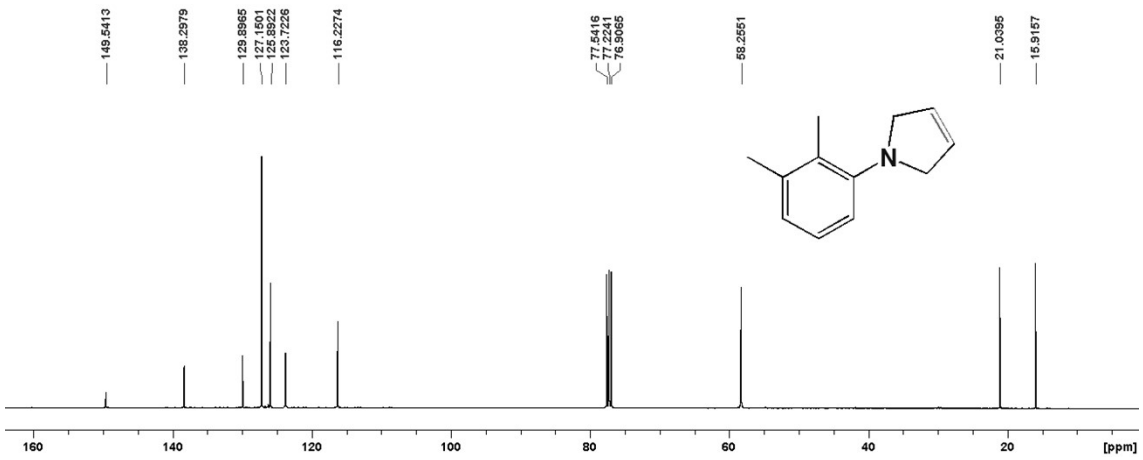

Figure S27. ^{13}C-NMR spectrum of **9i** in $CDCl_3$ at 25 ^{0}C.

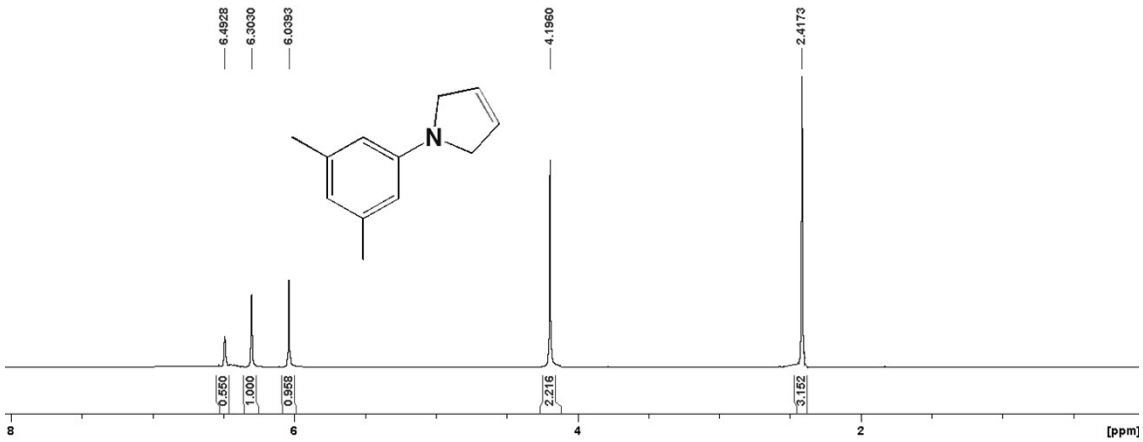

Figure S28. ^{1}H-NMR spectrum of **9j** in $CDCl_3$ at 25 ^{0}C.

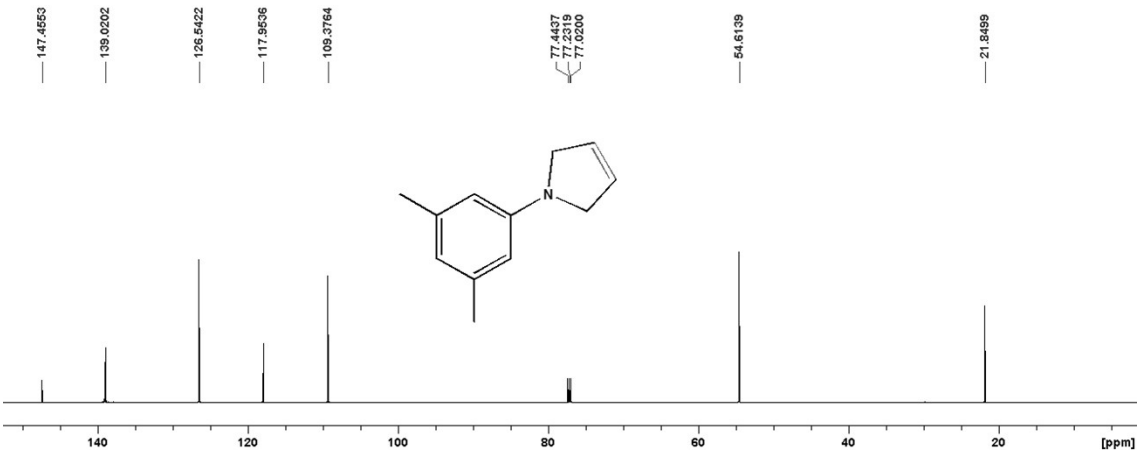

Figure S29. ^{13}C-NMR spectrum of **9j** in $CDCl_3$ at 25 ^{0}C.

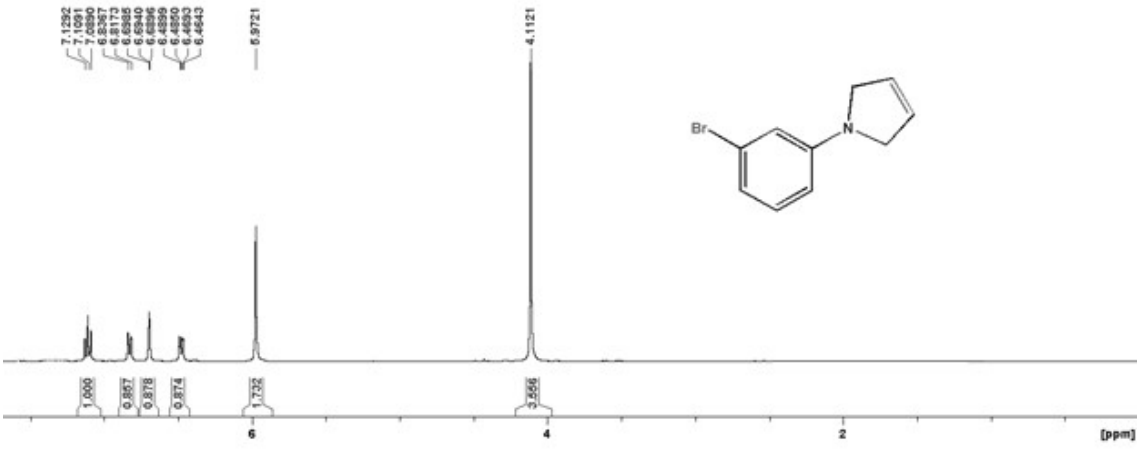

Figure S30. ^{1}H-NMR spectrum of **9l** in $CDCl_3$ at 25 ^{0}C.

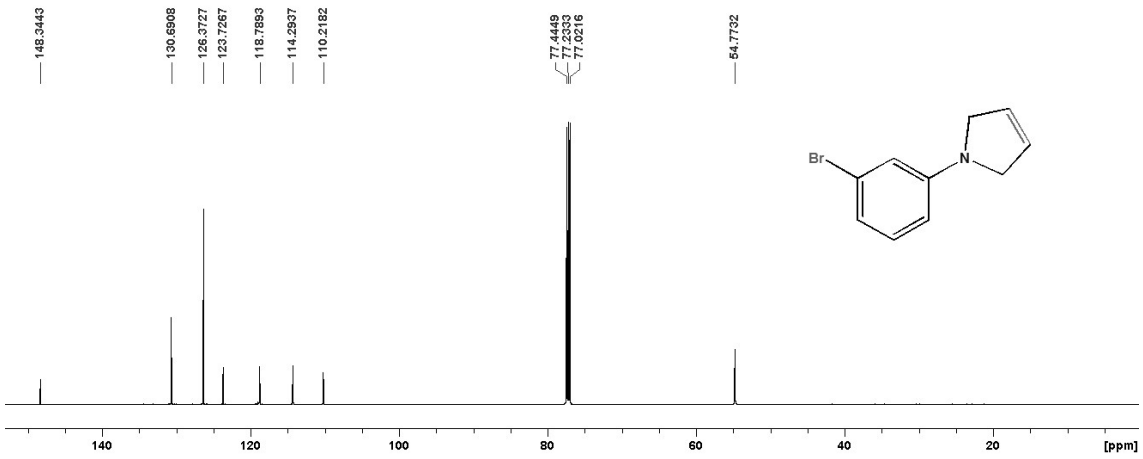

Figure S31. ^{13}C-NMR spectrum of **9l** in $CDCl_3$ at 25 ^{0}C.

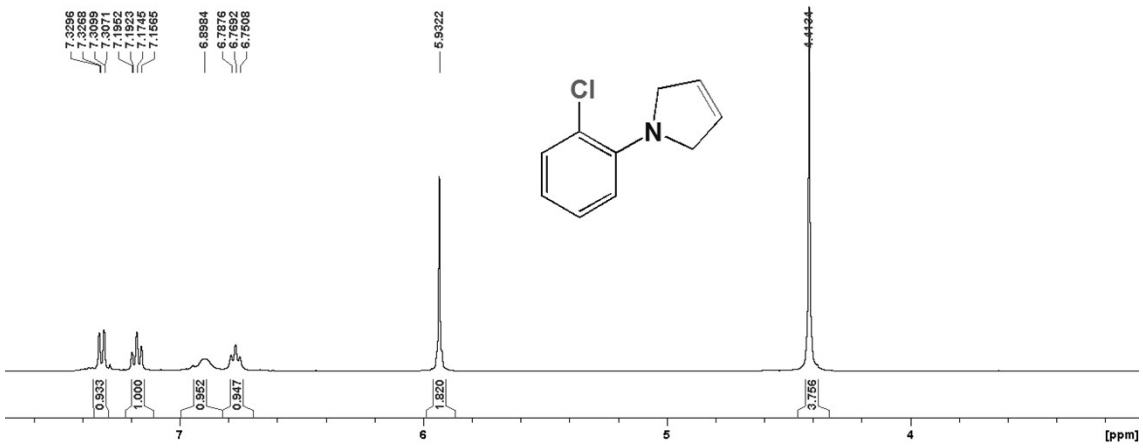

Figure S32. ^{1}H-NMR spectrum of **9m** in $CDCl_3$ at 25 ^{0}C.

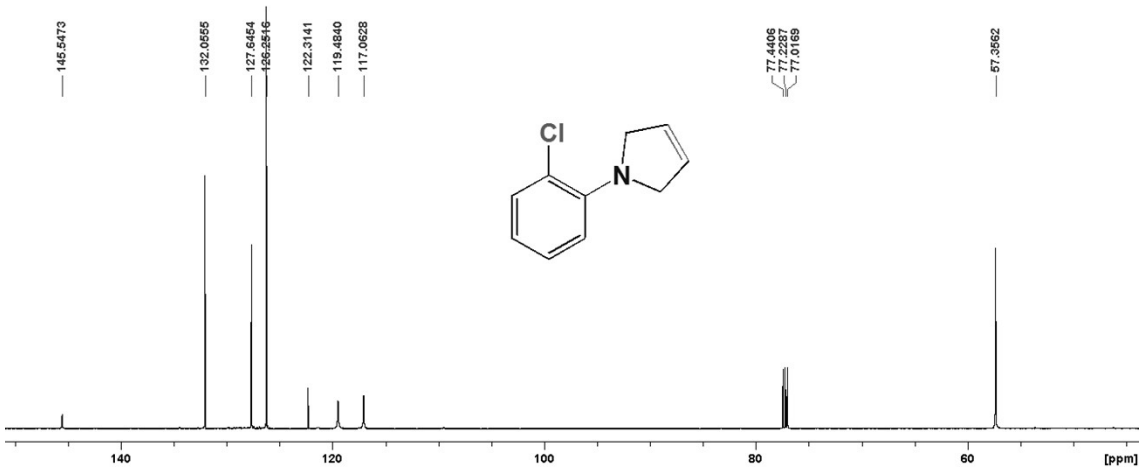

Figure S33. ^{13}C-NMR spectrum of **9m** in $CDCl_3$ at 25 ^{0}C.

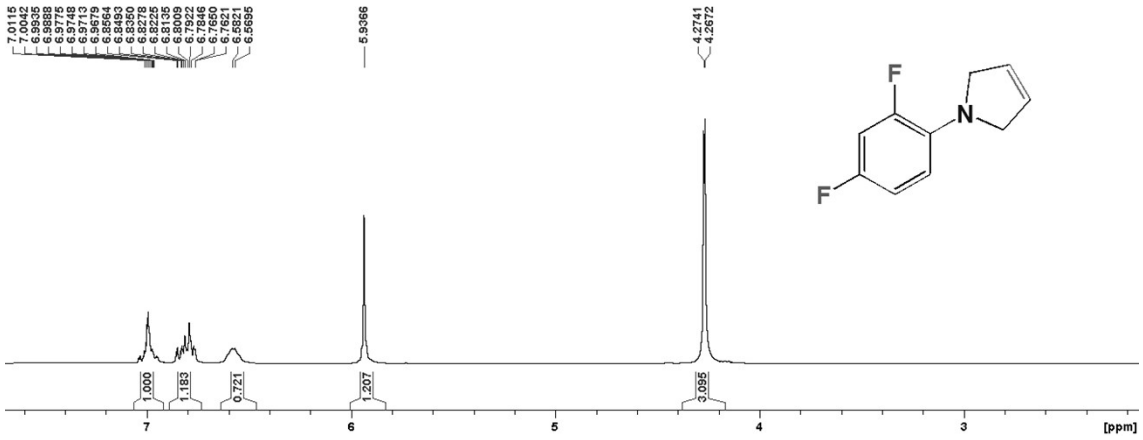

Figure S34. ^{1}H-NMR spectrum of **9o** in $CDCl_3$ at 25 ^{0}C.

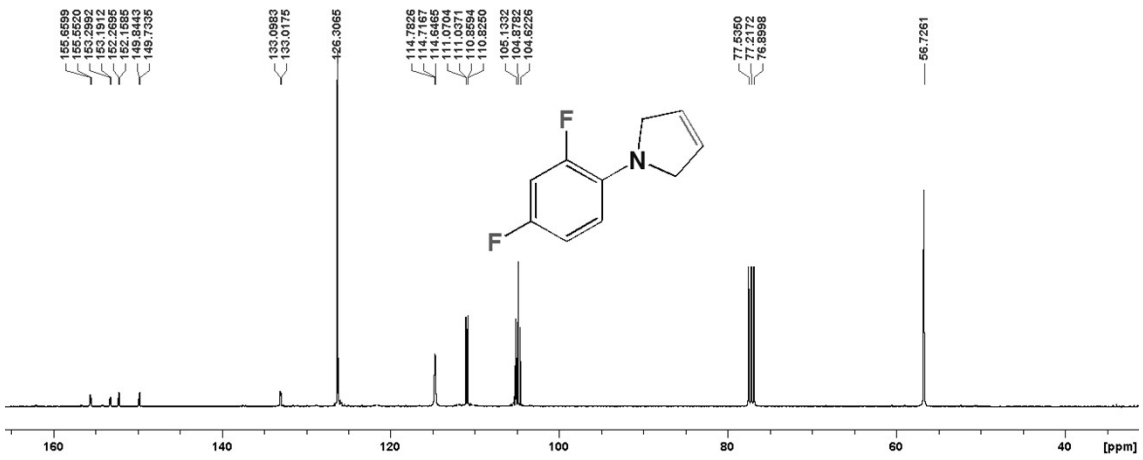

Figure S35. ^{13}C-NMR spectrum of **9o** in $CDCl_3$ at 25 ^{0}C.

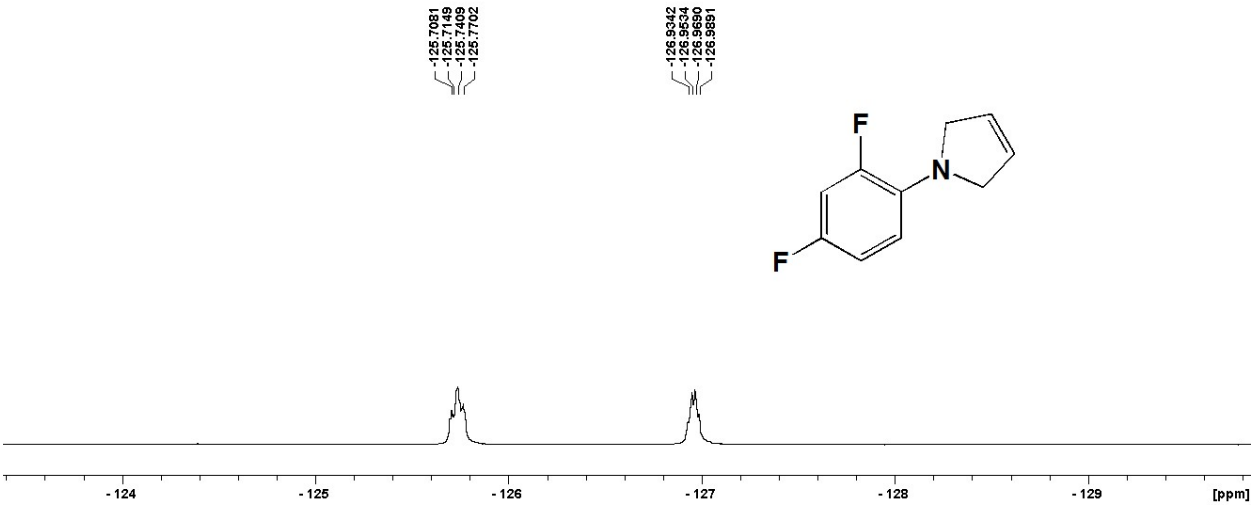

Figure S36. 19F NMR spectrum of **9o** in $CDCl_3$ at 25 ^{0}C.

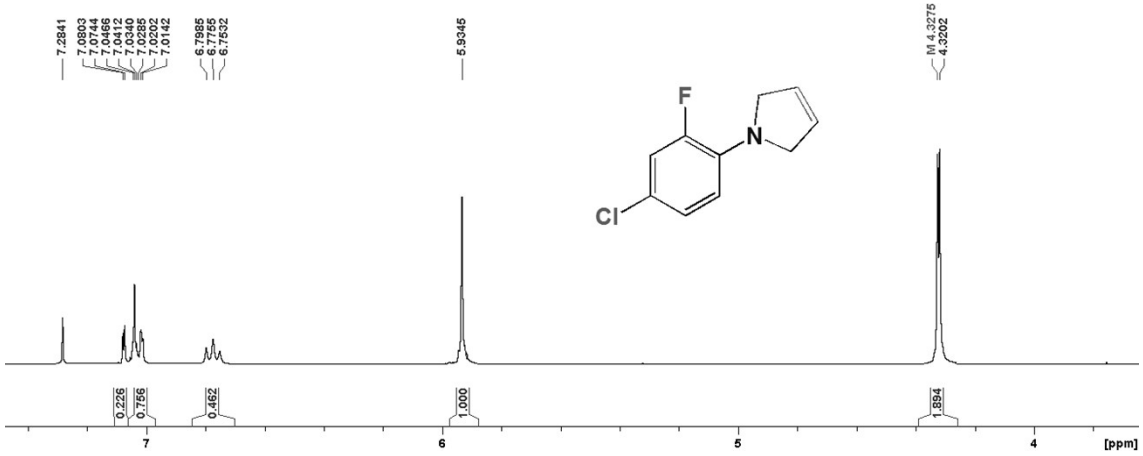

Figure S37. ^{1}H-NMR spectrum of **9q** in $CDCl_3$ at 25 ^{0}C.

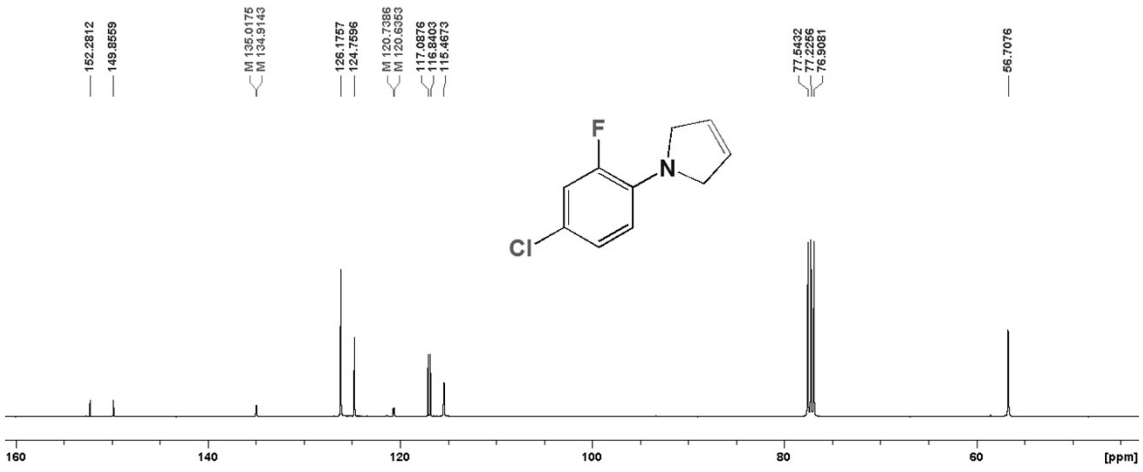

Figure S38. ^{13}C-NMR spectrum of **9q** in $CDCl_3$ at 25 ^{0}C.

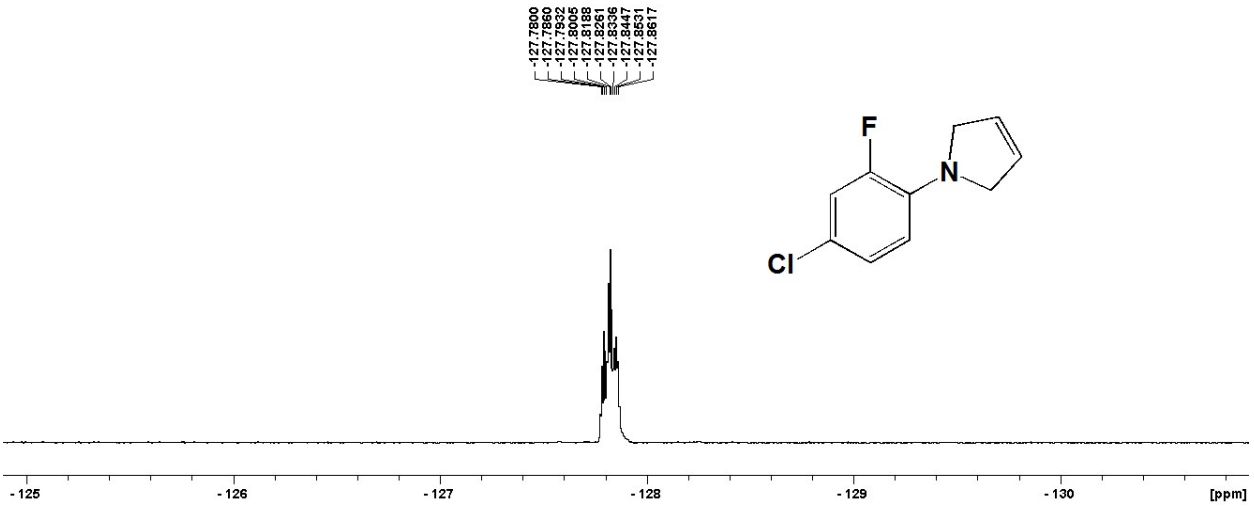

Figure S39. 19F NMR spectrum of **9q** in $CDCl_3$ at 25 ^{0}C.

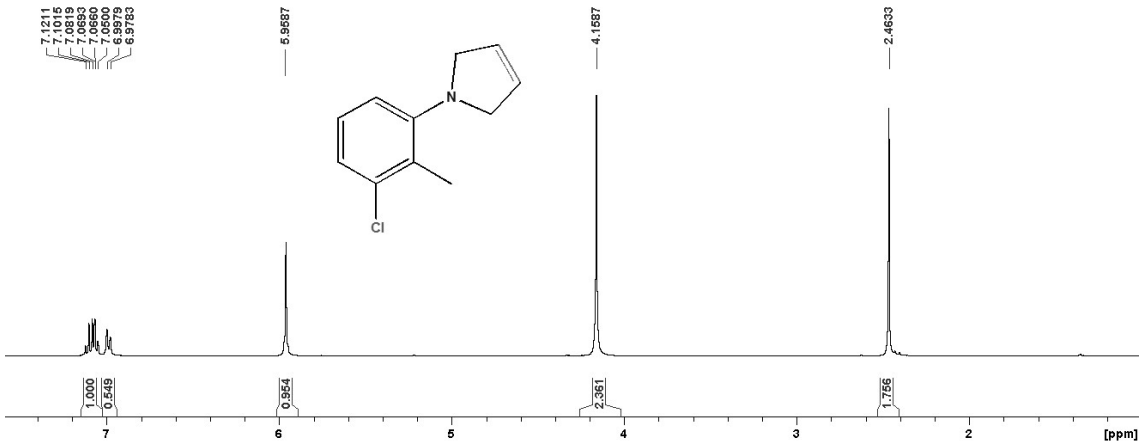

Figure S40. ^{1}H-NMR spectrum of **9r** in $CDCl_3$ at 25 ^{0}C.

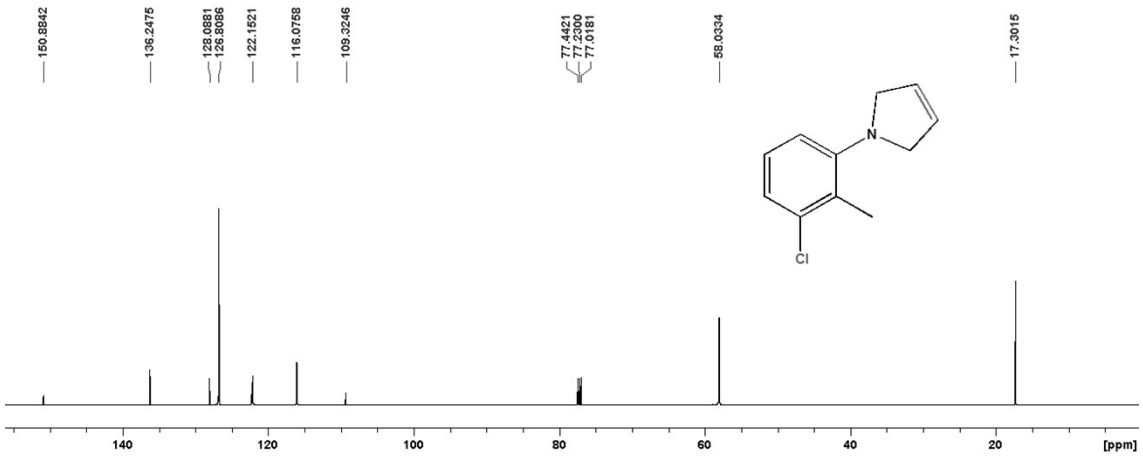

Figure S41. ^{13}C-NMR spectrum of **9r** in $CDCl_3$ at 25 ^{0}C.

Mass spectra

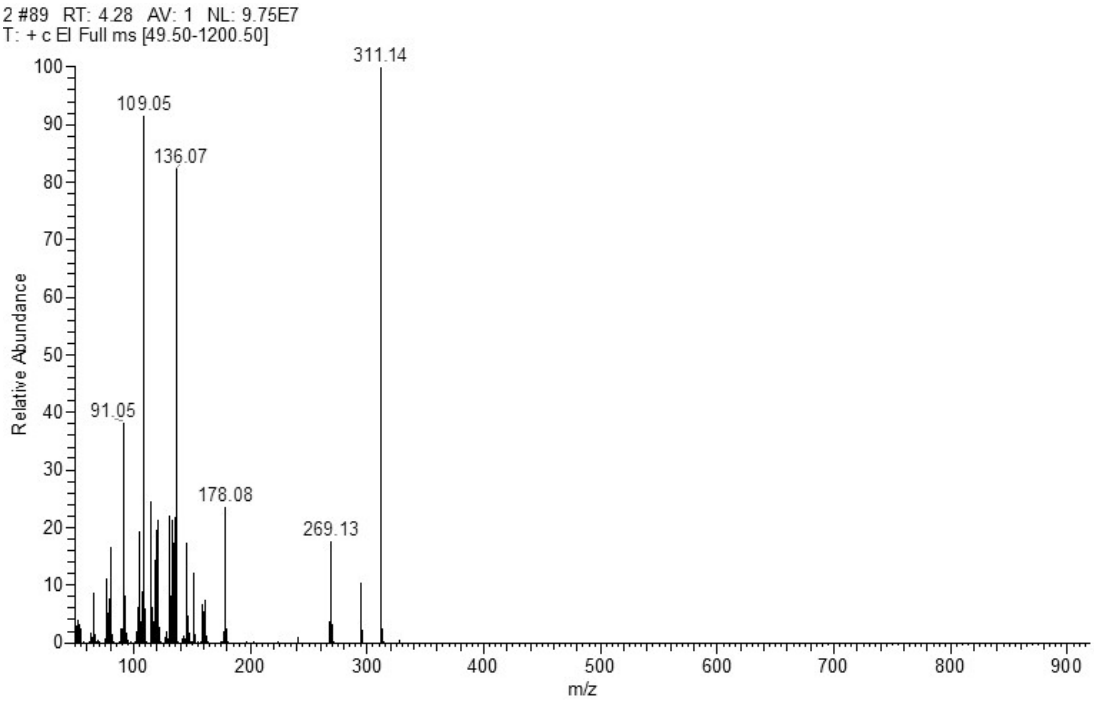

Figure S42. EI spectrum of **6a**.

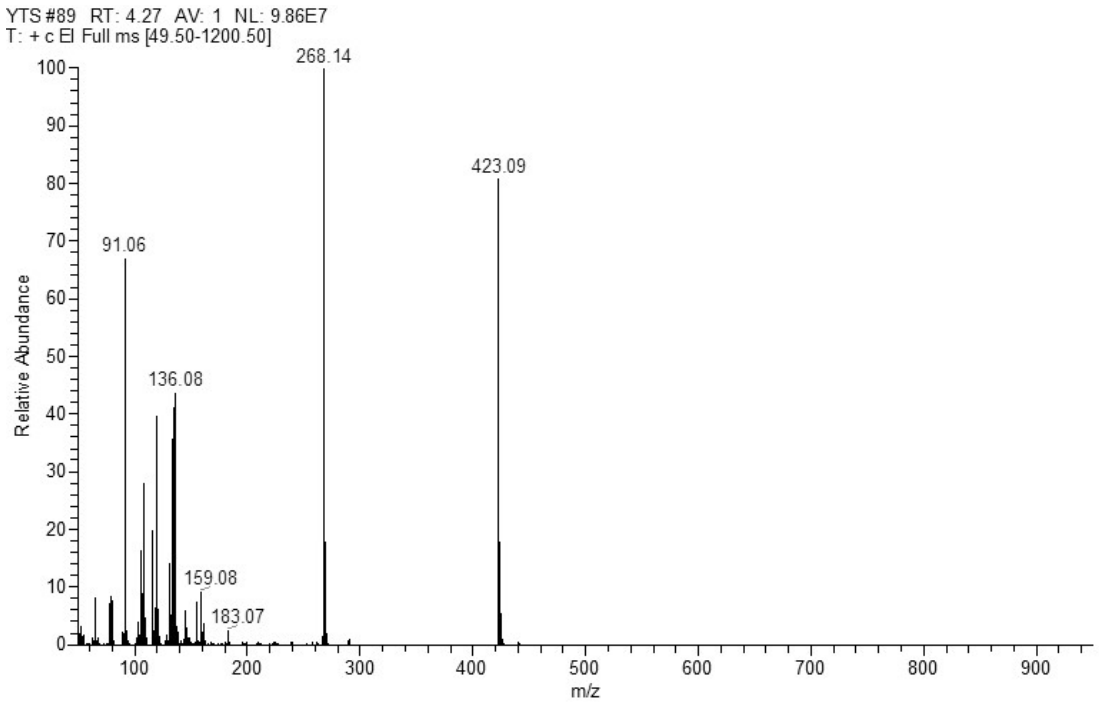

Figure S43. EI spectrum of **6b**.

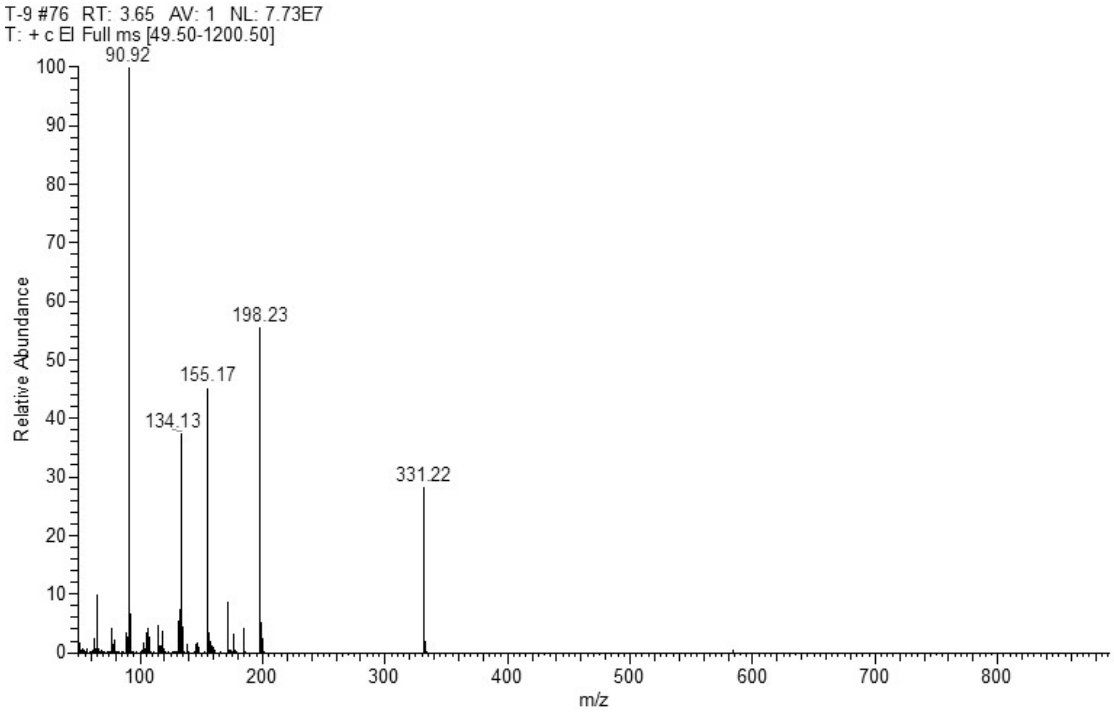

Figure S44. EI spectrum of **6c**.

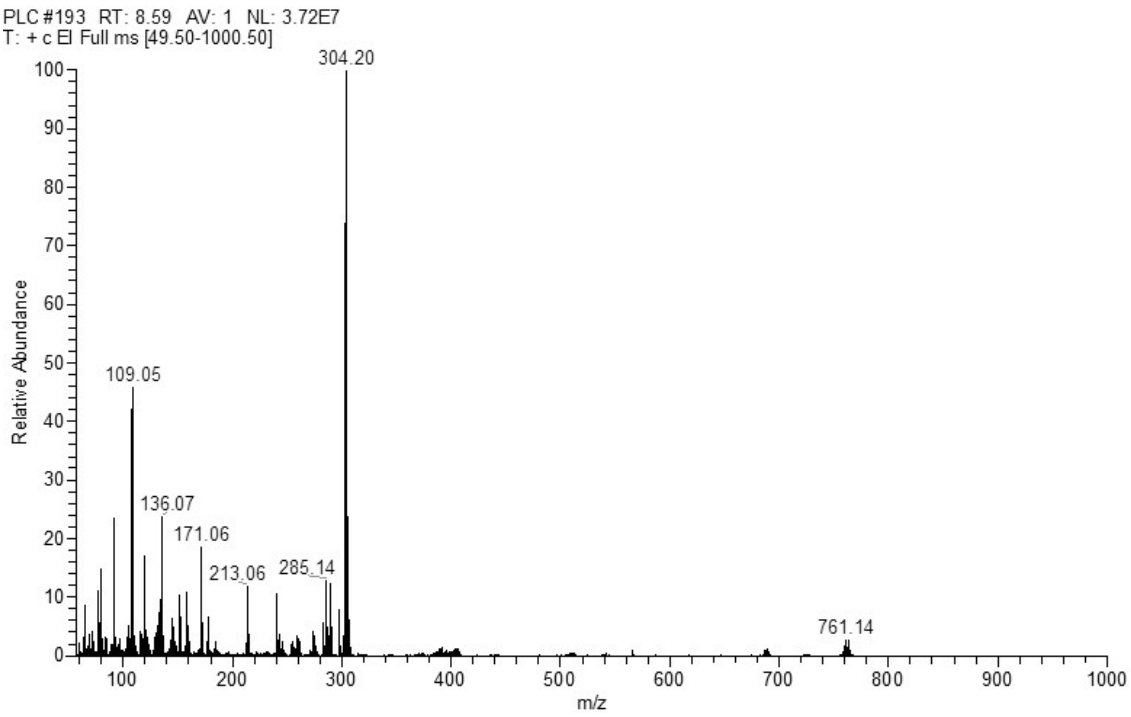

Figure S45. EI spectrum of **7a**.

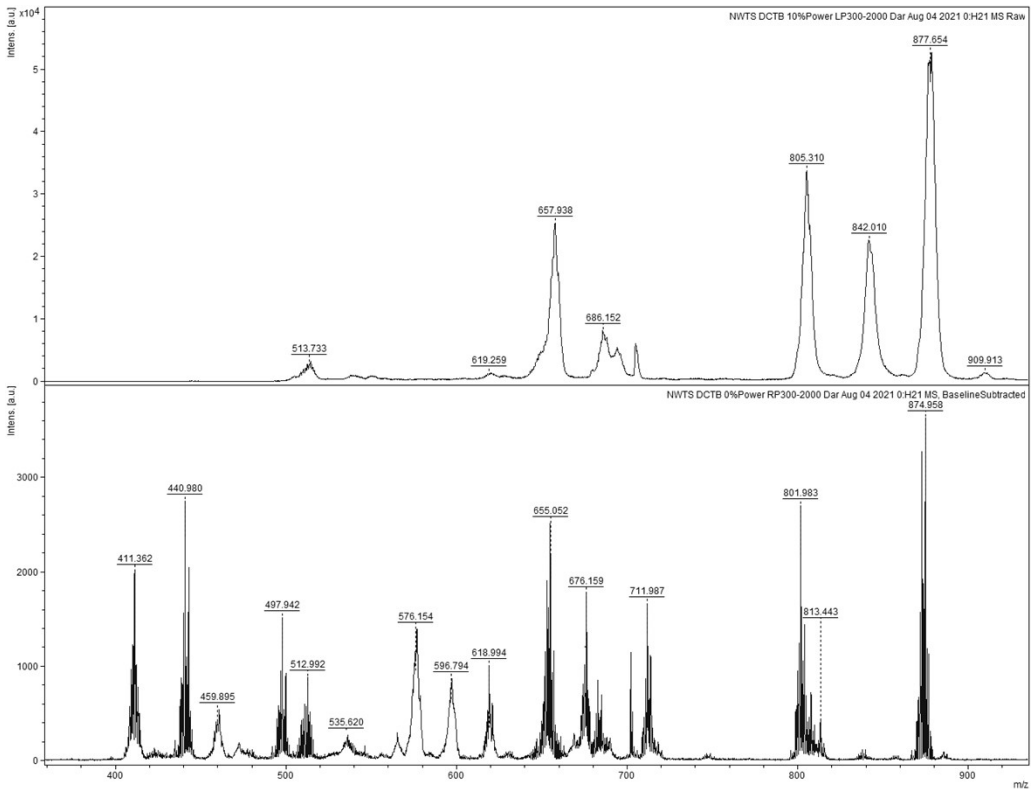

Figure S46. MALDI-MS spectrum of **7b**.

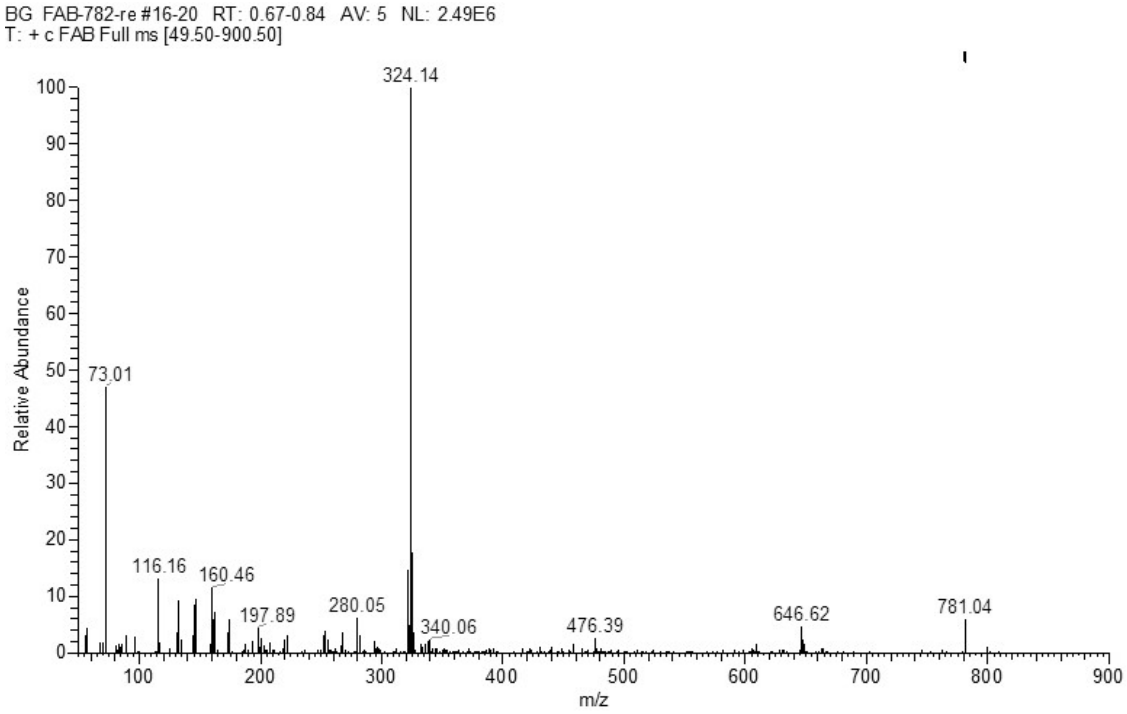

Figure S47. FAB-MS spectrum of **7c**.

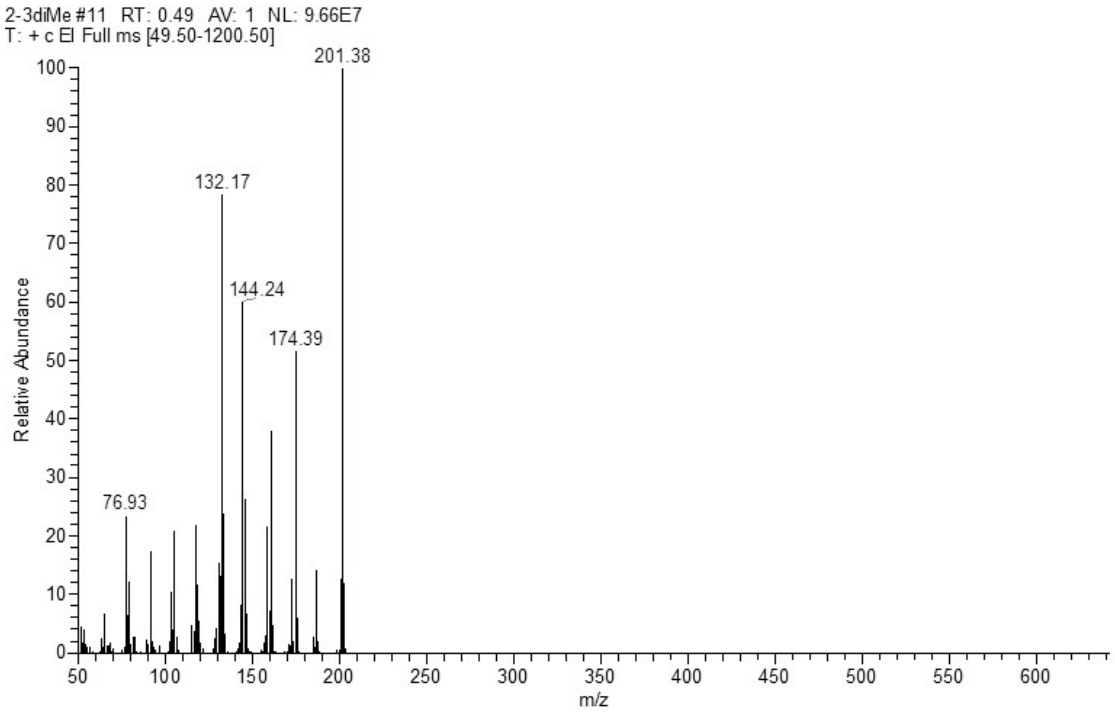

Figure S48. EI spectrum of **8i**.

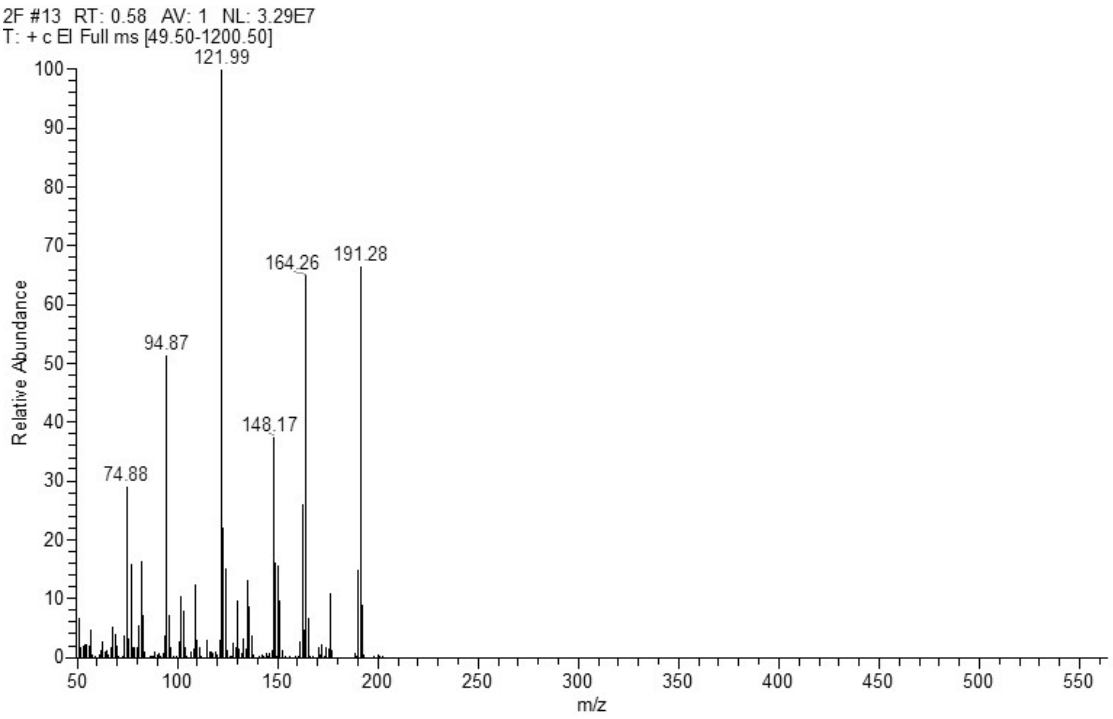

Figure S49. EI spectrum of **8k**.

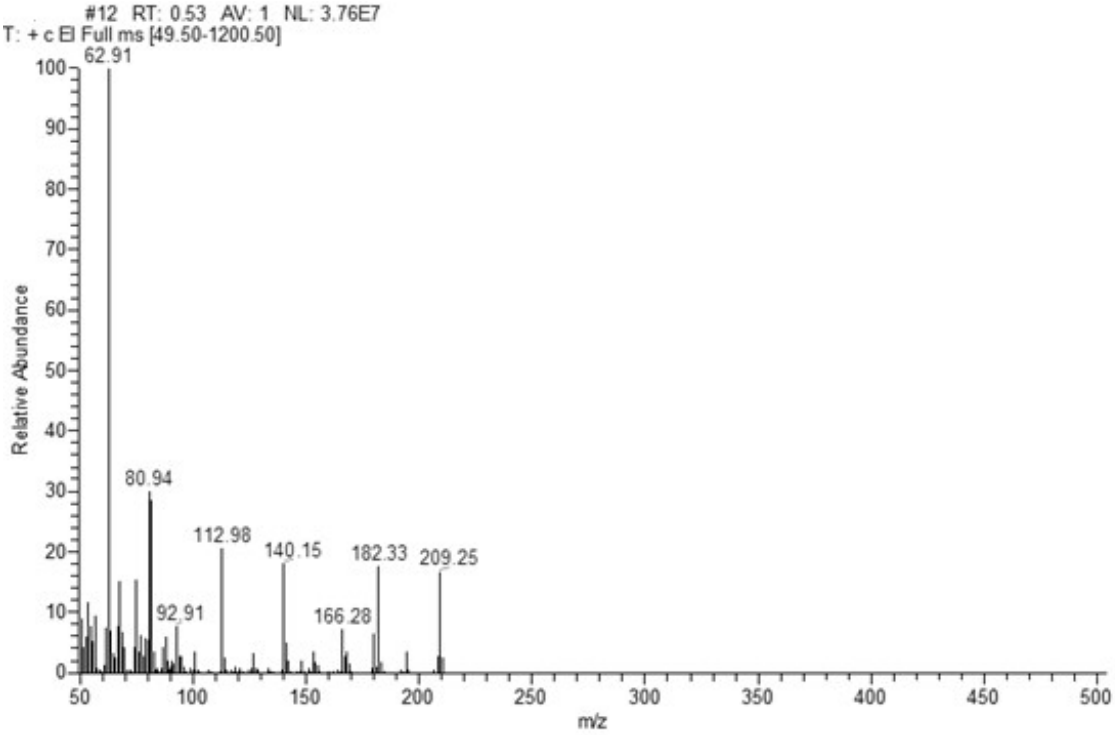

Figure S50. EI spectrum of **8o**.

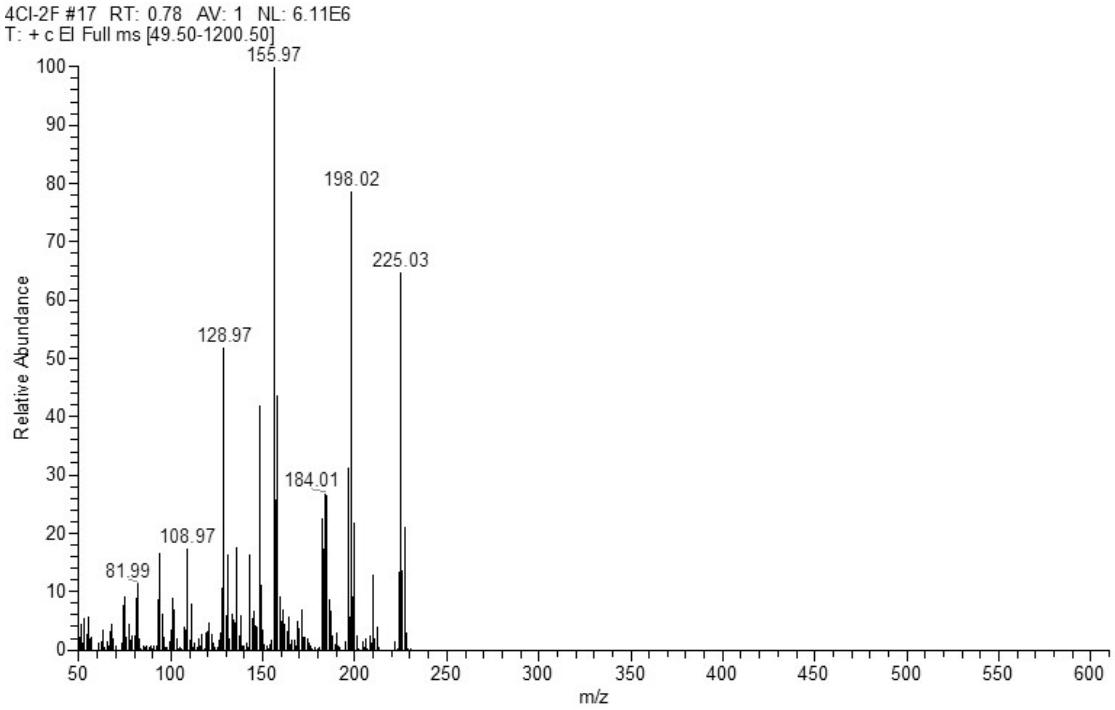

Figure S51. EI spectrum of **8q**.

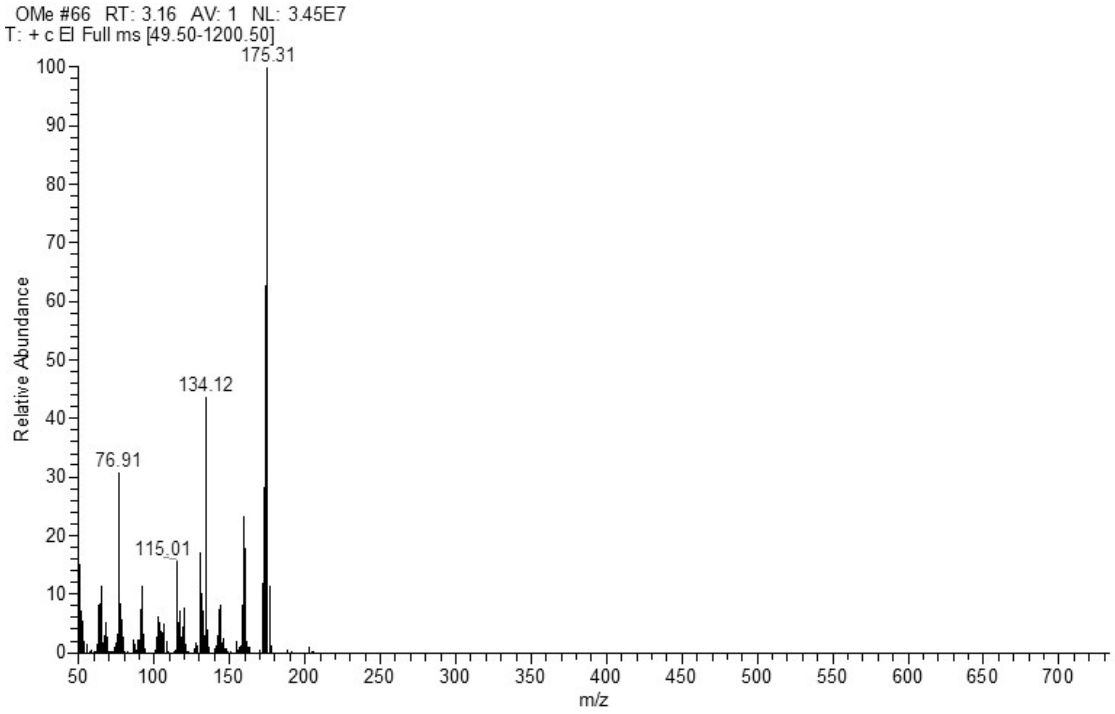

Figure S52. EI spectrum of **9f**.

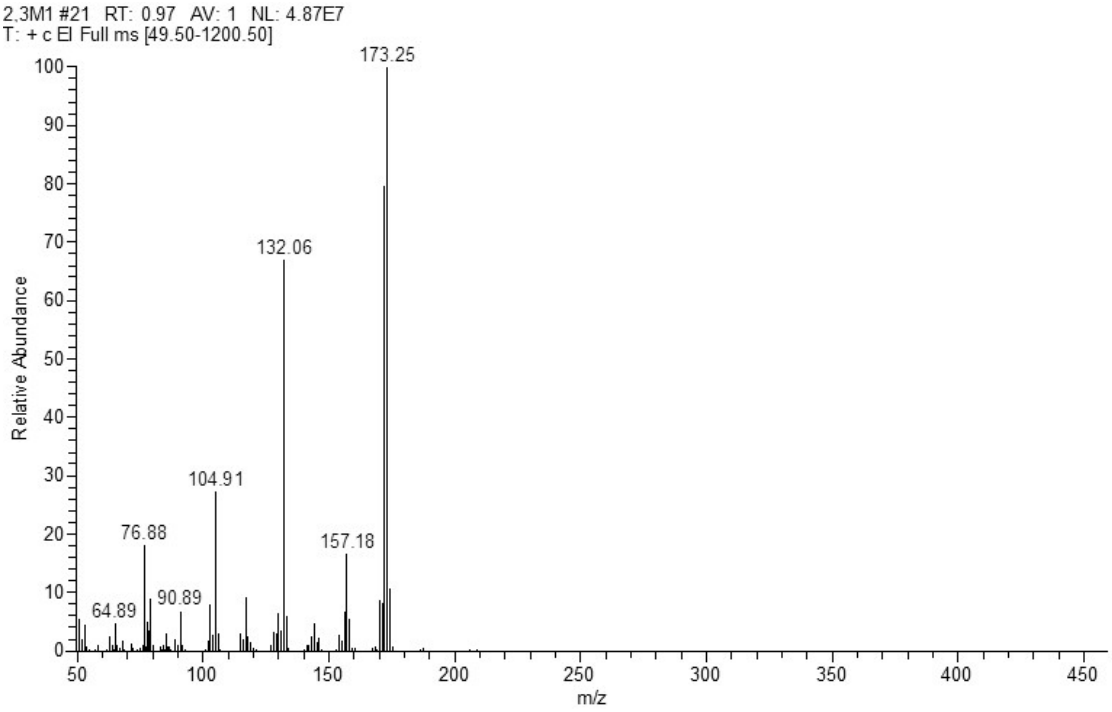

Figure S53. EI spectrum of **9i**.

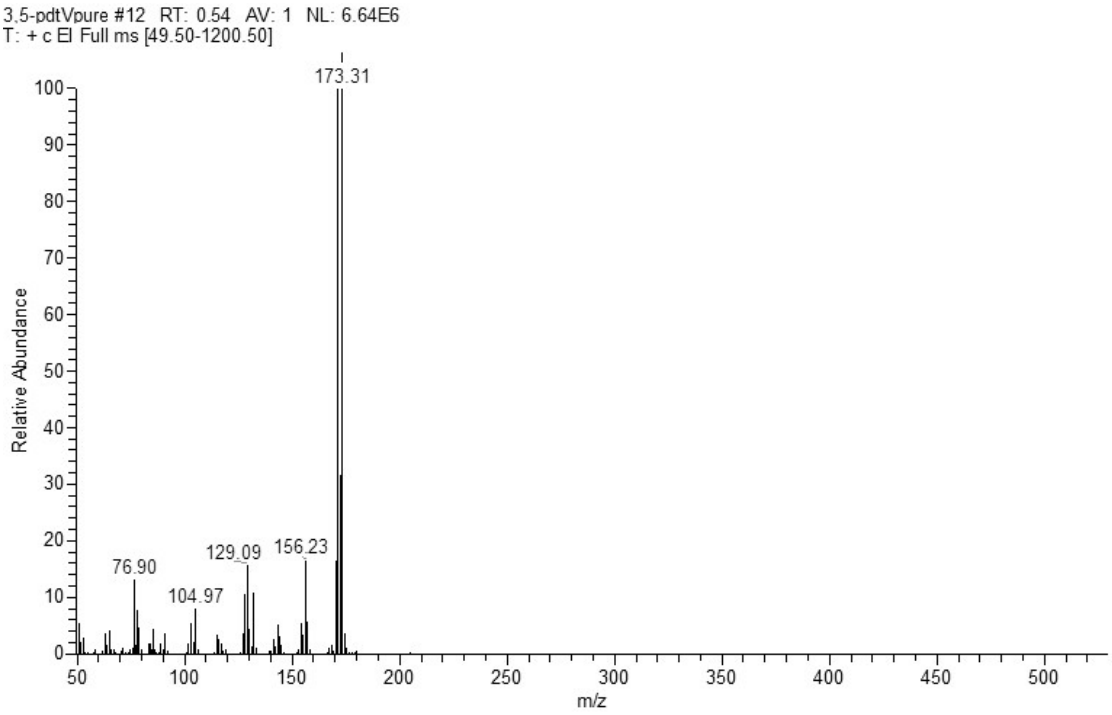

Figure S54. EI spectrum of **9j**.

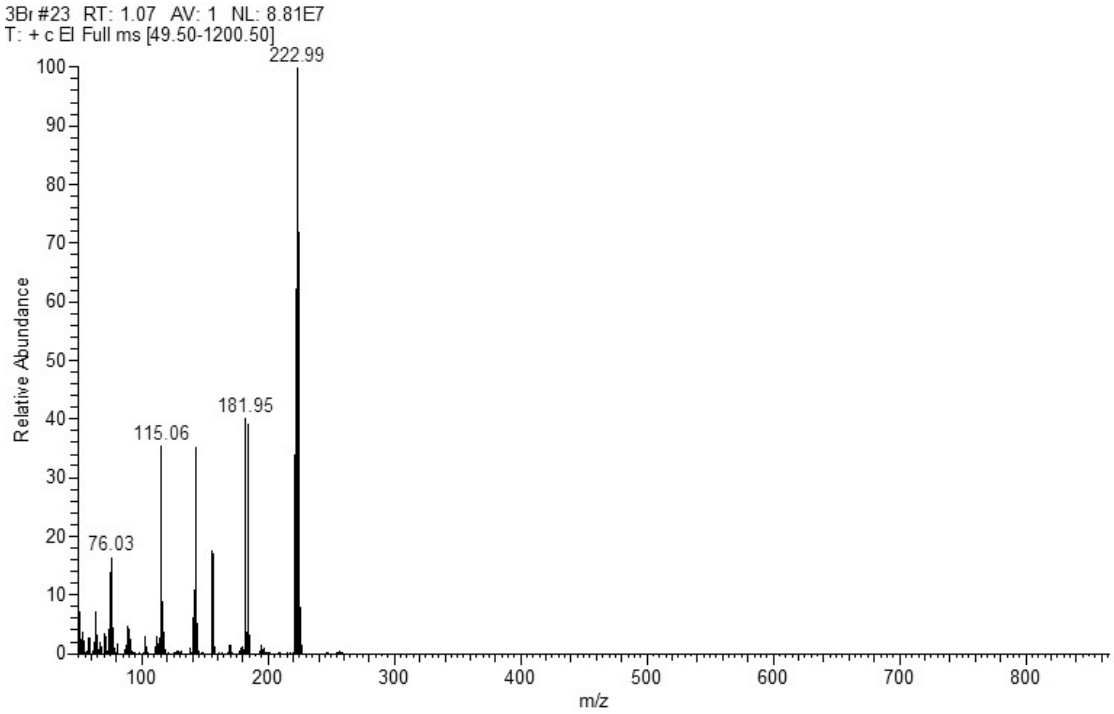

Figure S55. EI spectrum of **9l**.

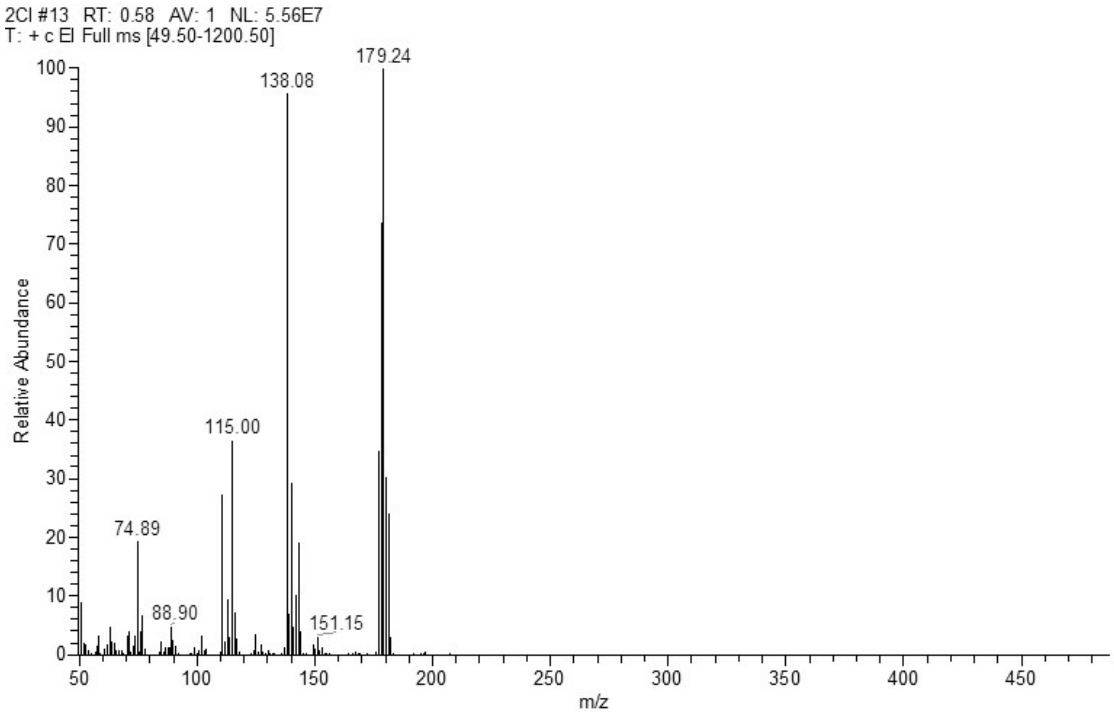

Figure S56. EI spectrum of **9m**.

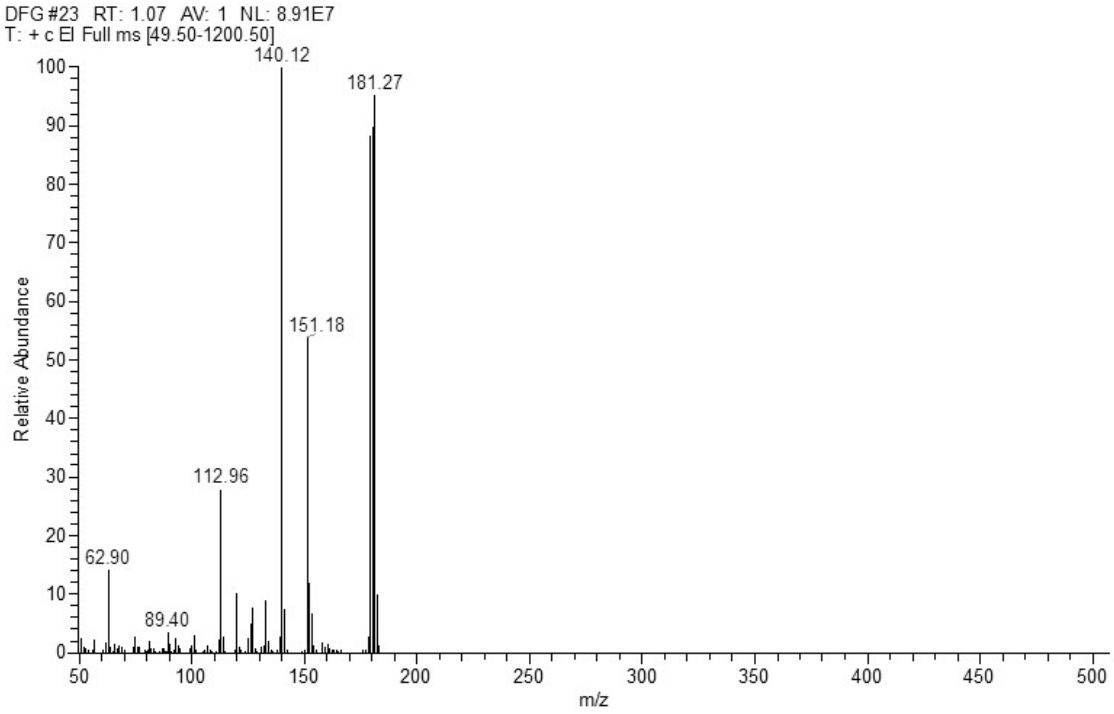

Figure S57. EI spectrum of **9o**.

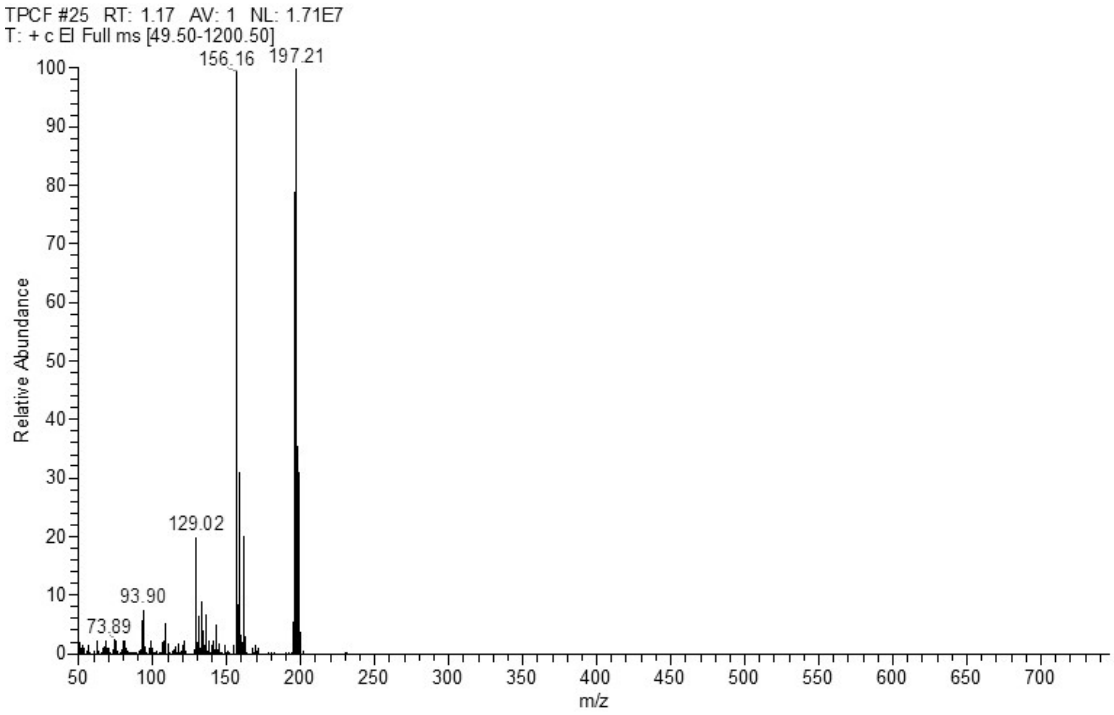

Figure S58. EI spectrum of **9q**.

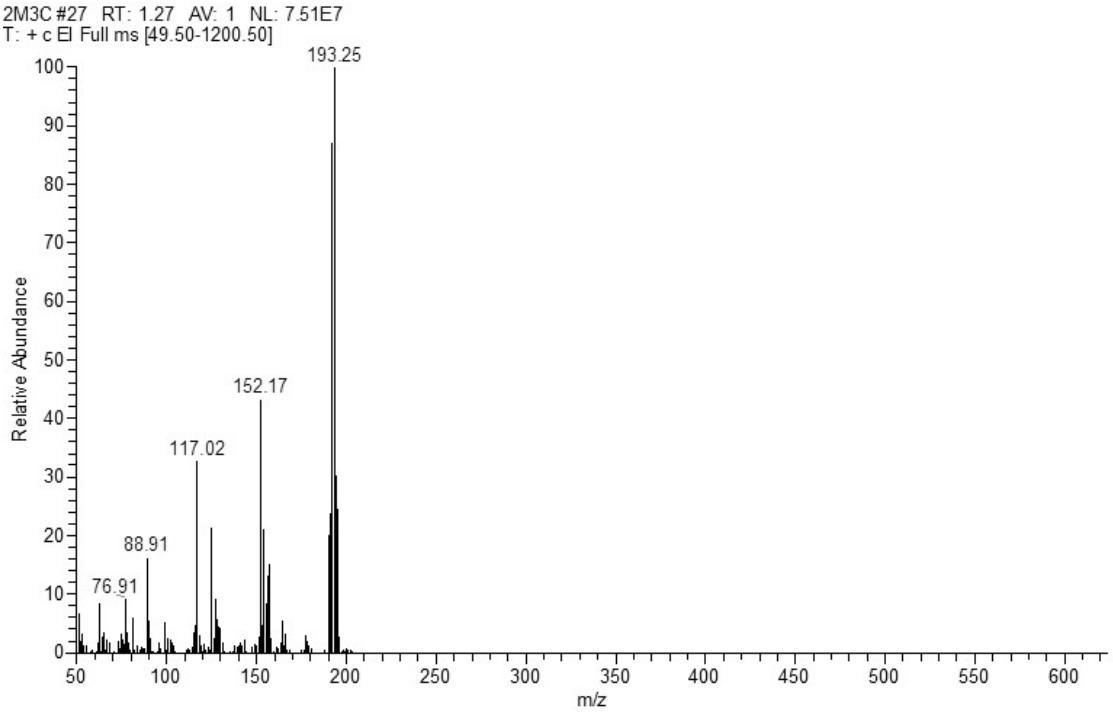

Figure S59. EI spectrum of **9r**.

Deconvoluted HRMS (ESI)

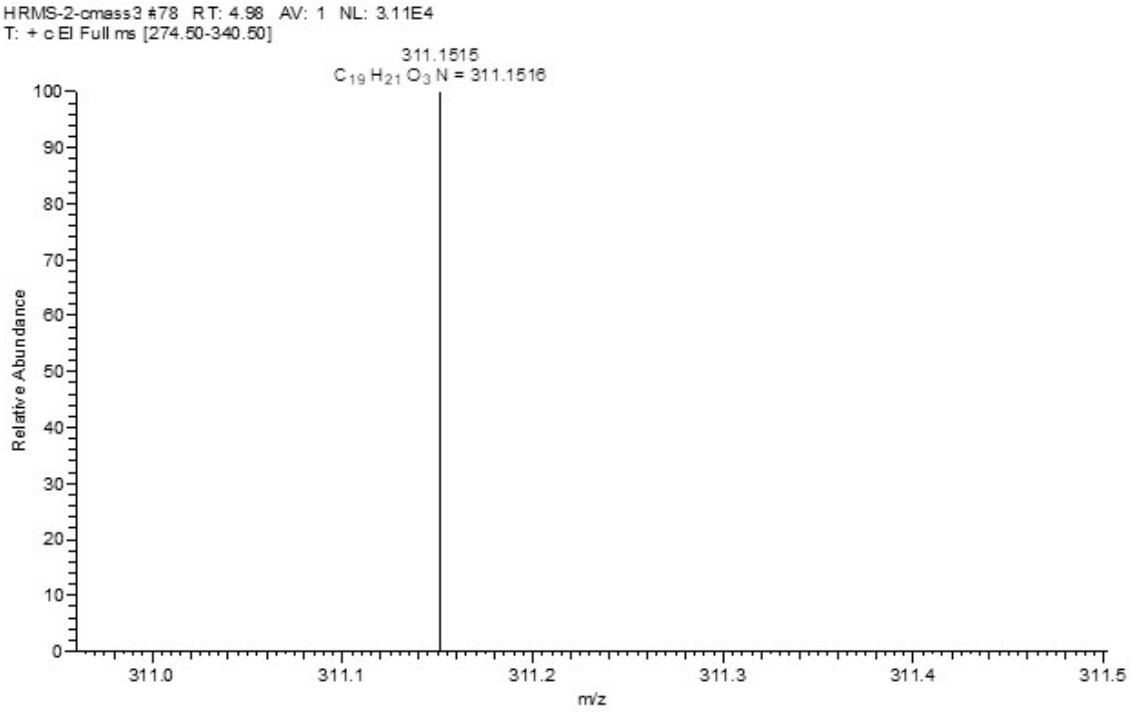

Figure S60. HRMS spectrum of **6a**.

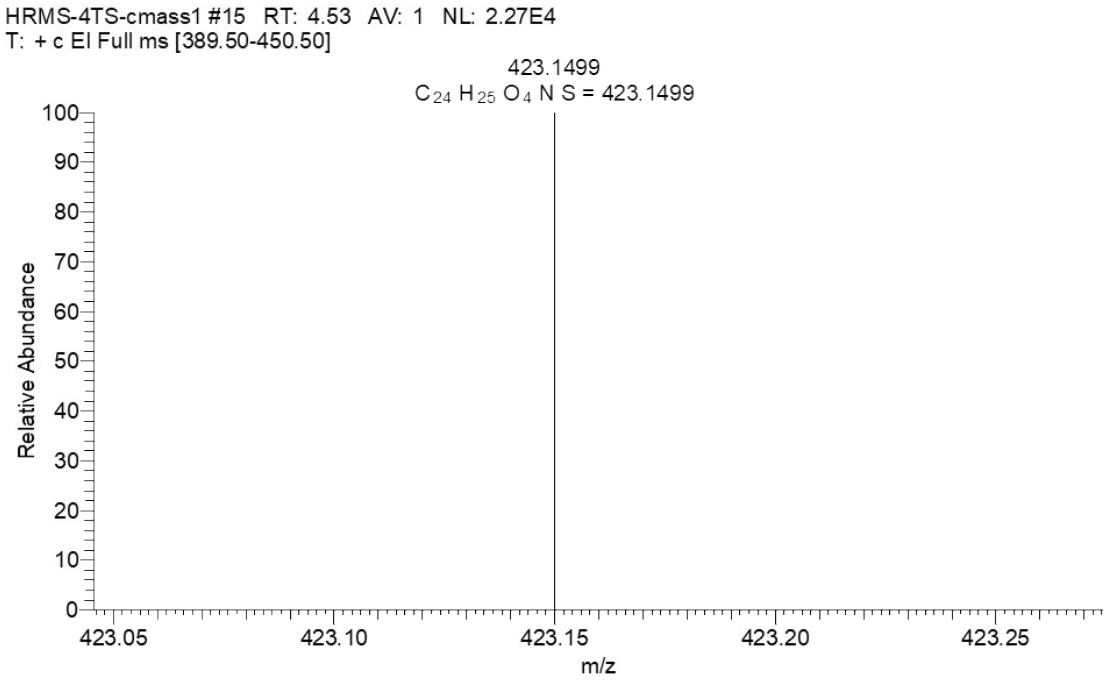

Figure S61. HRMS spectrum of **6b**.

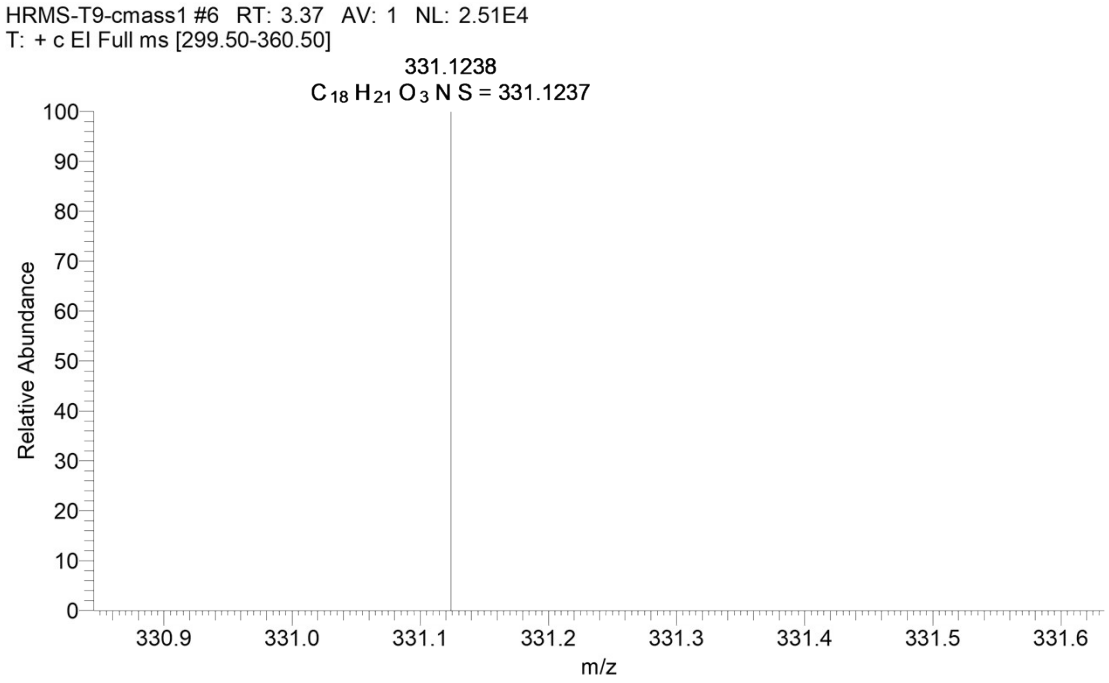

Figure S62. HRMS spectrum of **6c**.

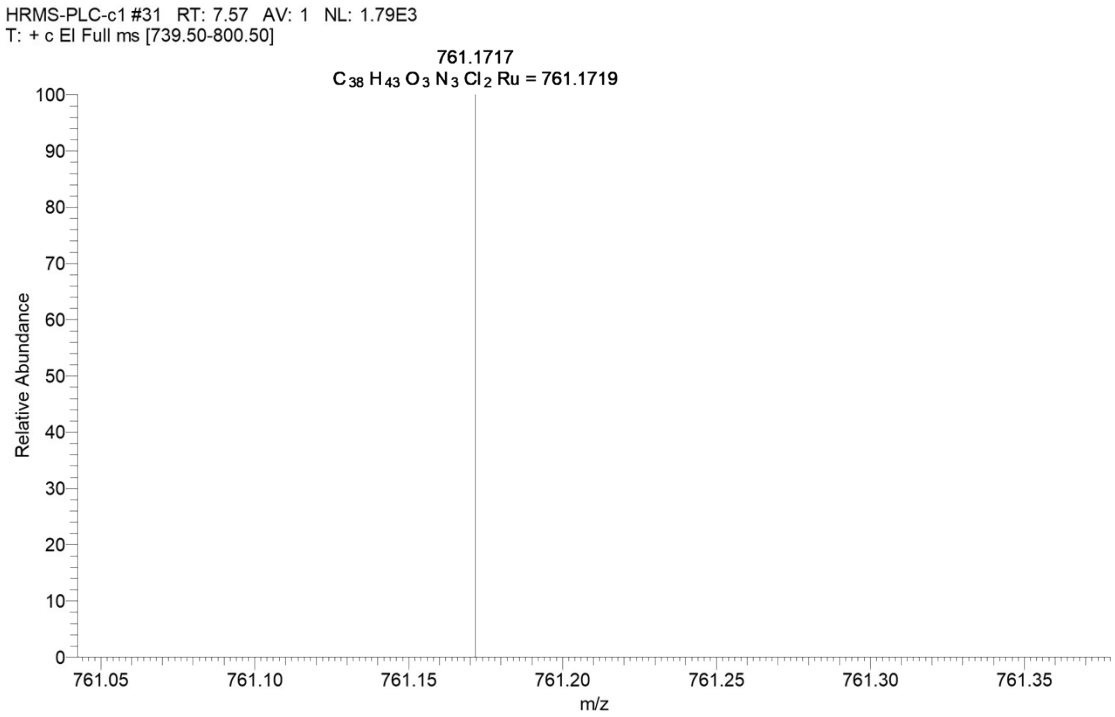

Figure S63. HRMS spectrum of **7a**.

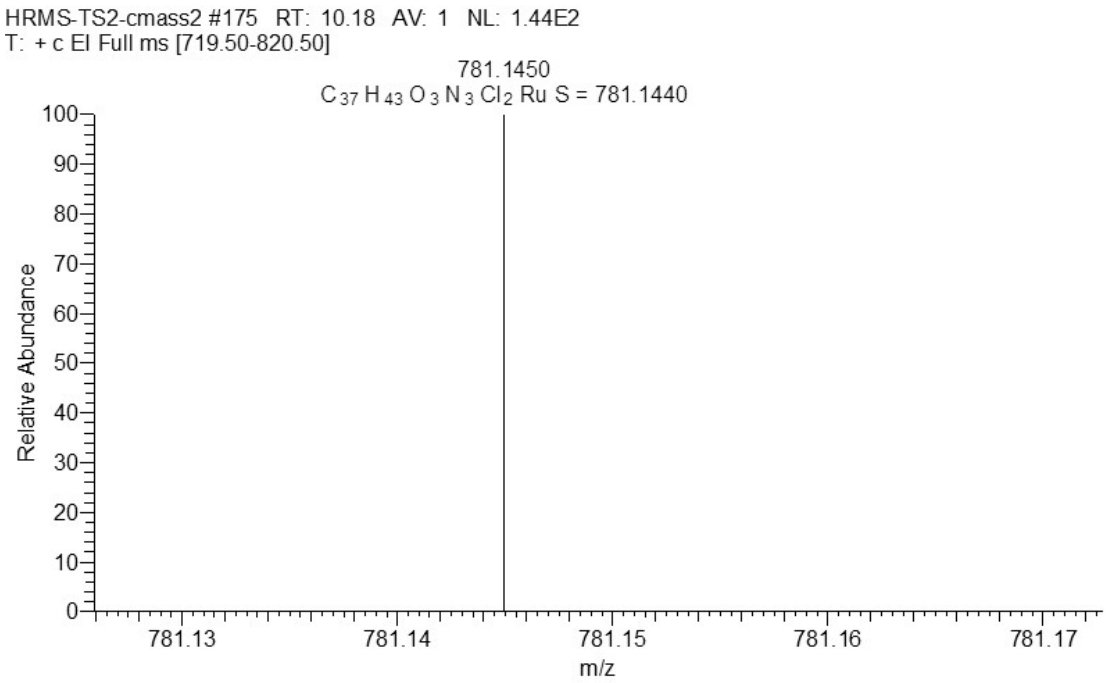

Figure S64. HRMS spectrum of **7c**.

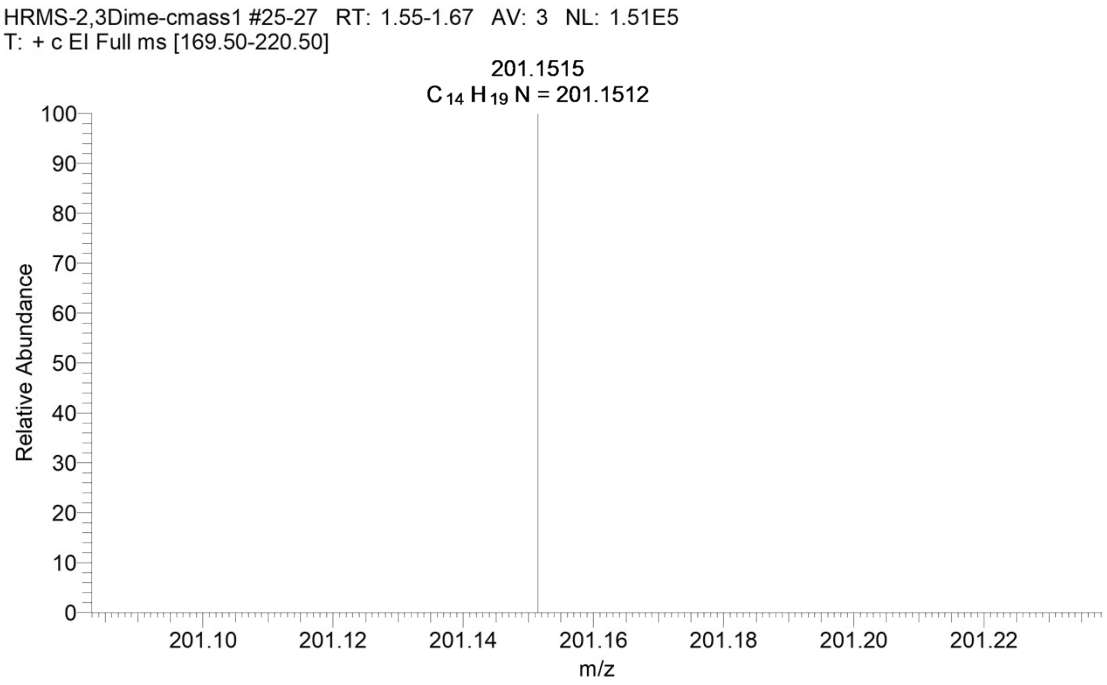

Figure S65. HRMS spectrum of **8i**.

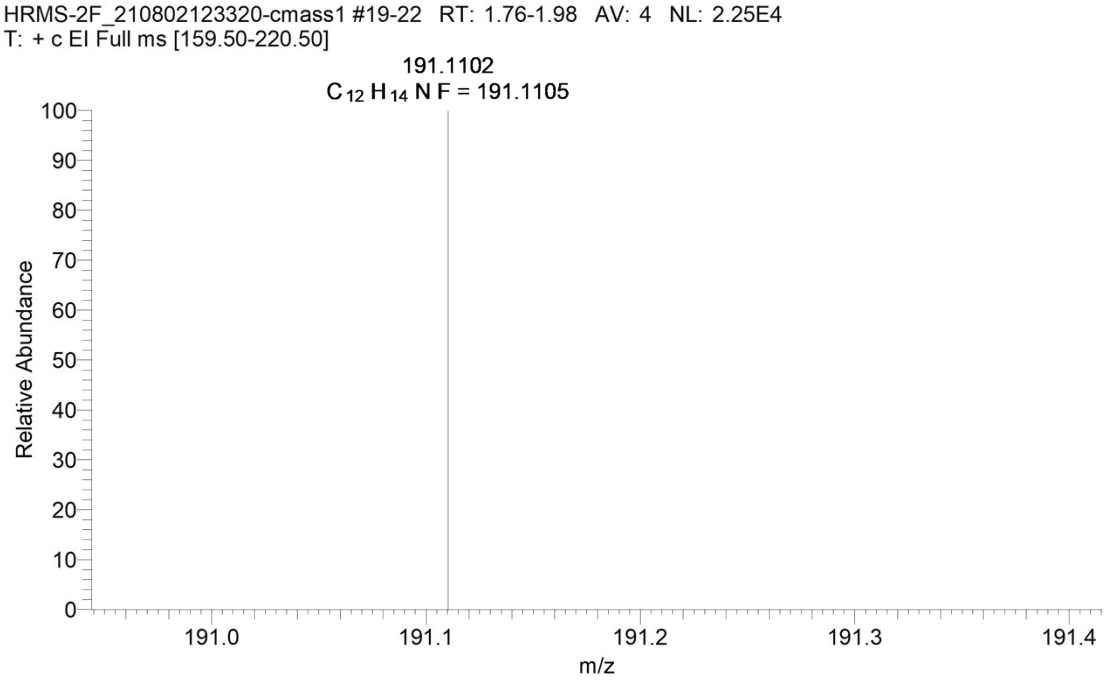

Figure S66. HRMS spectrum of **8k**.

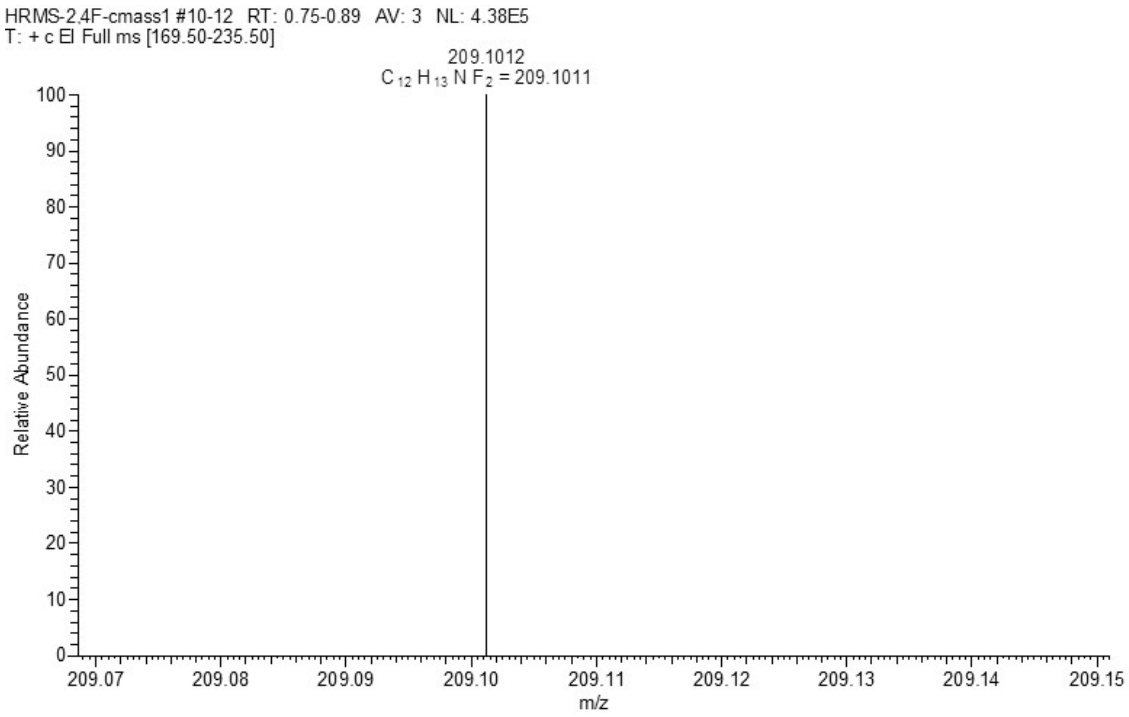

Figure S67. HRMS spectrum of **8o**.

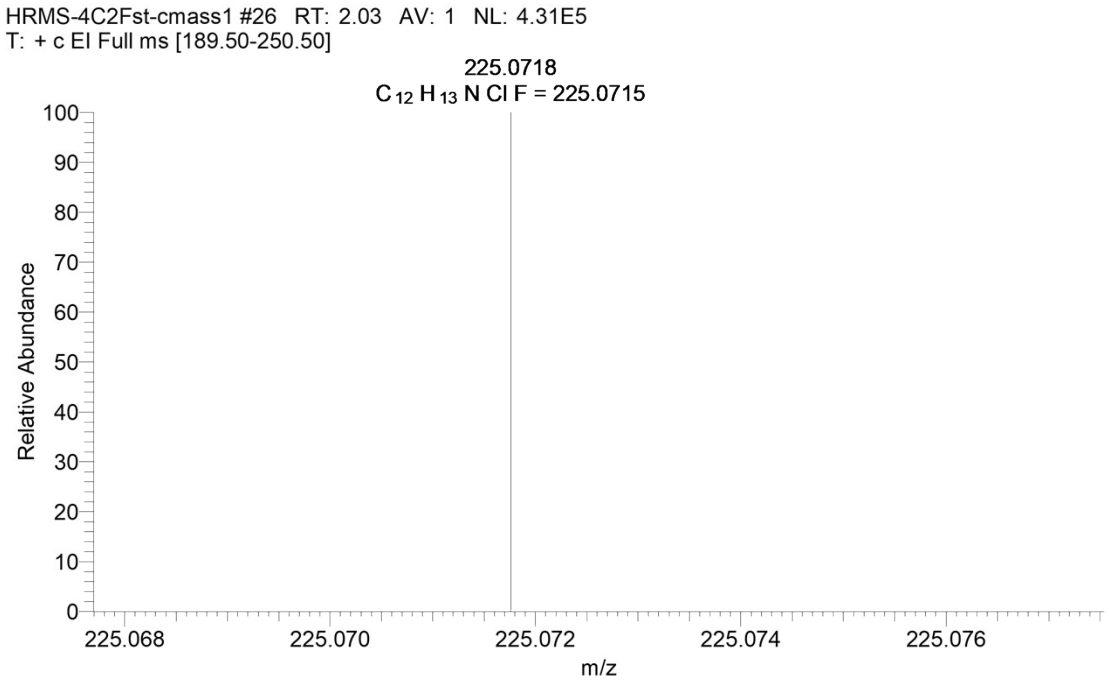

Figure S68. HRMS spectrum of **8q**.

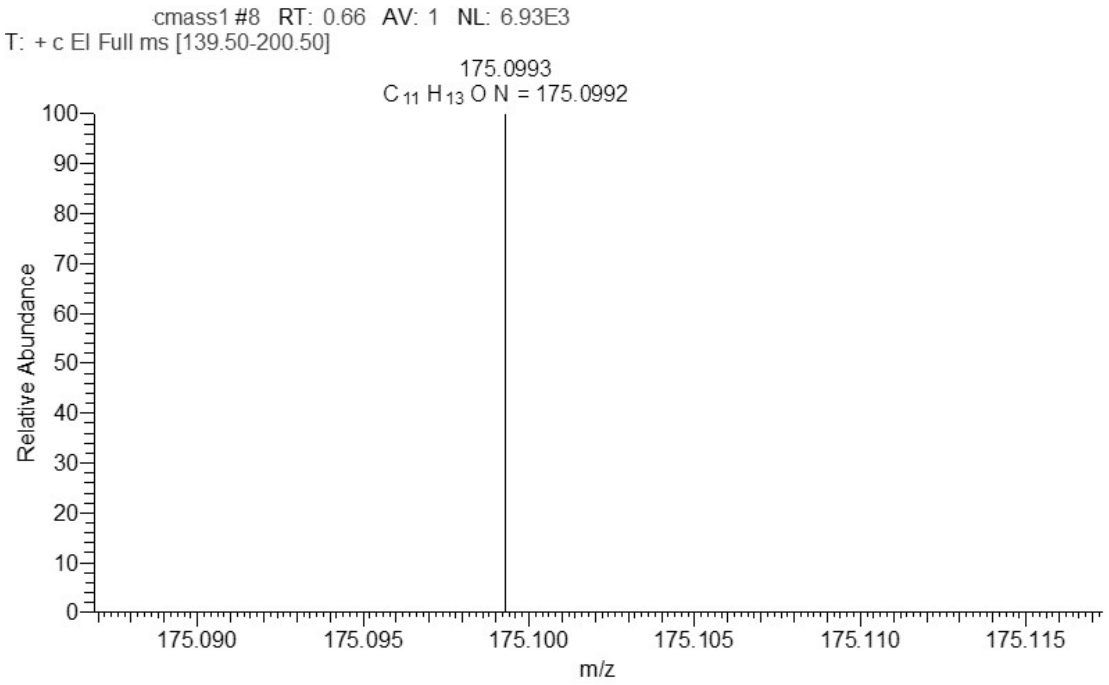

Figure S69. HRMS spectrum of **9f**.

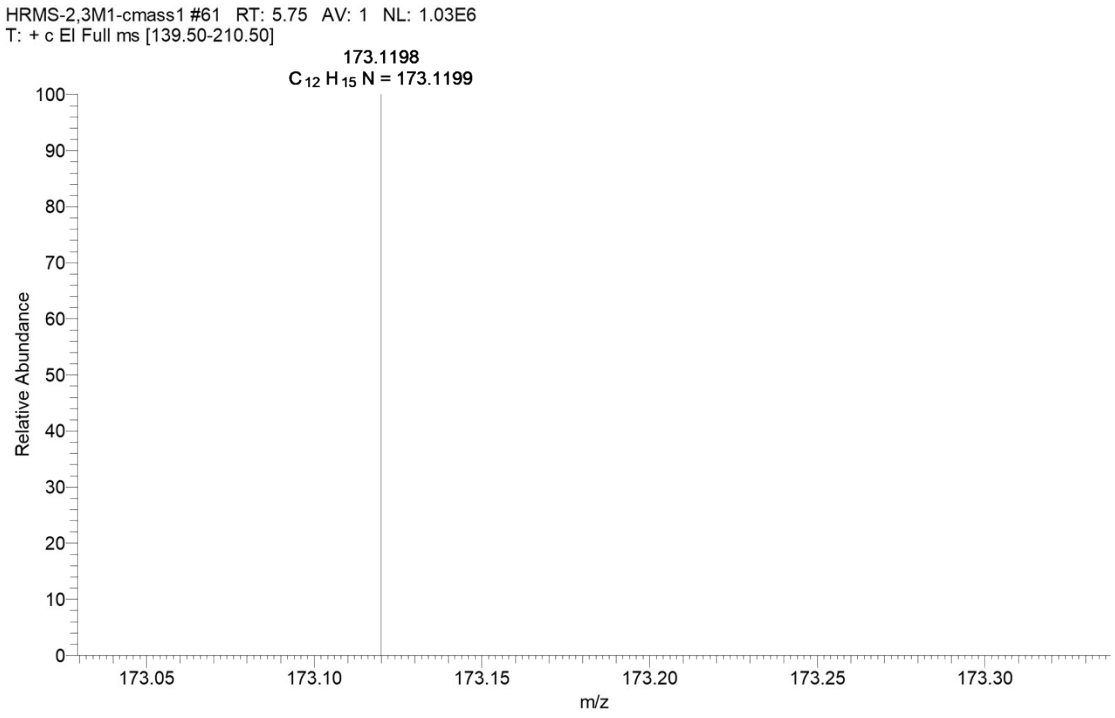

Figure S70. HRMS spectrum of **9i**.

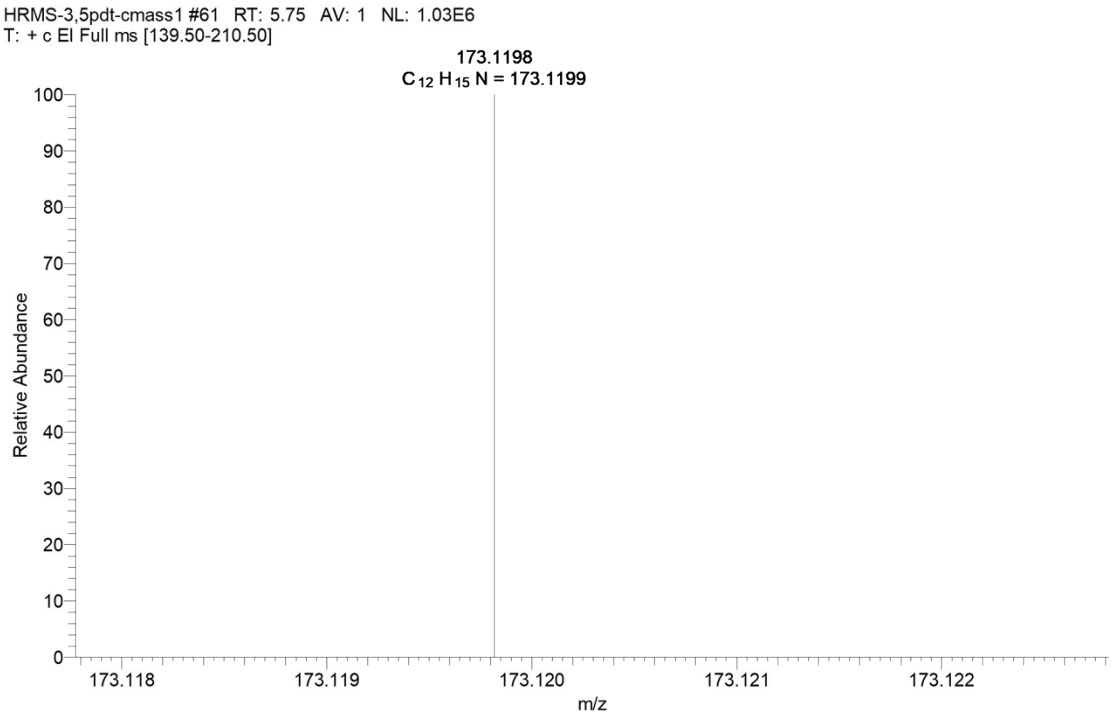

Figure S71. HRMS spectrum of **9j**.

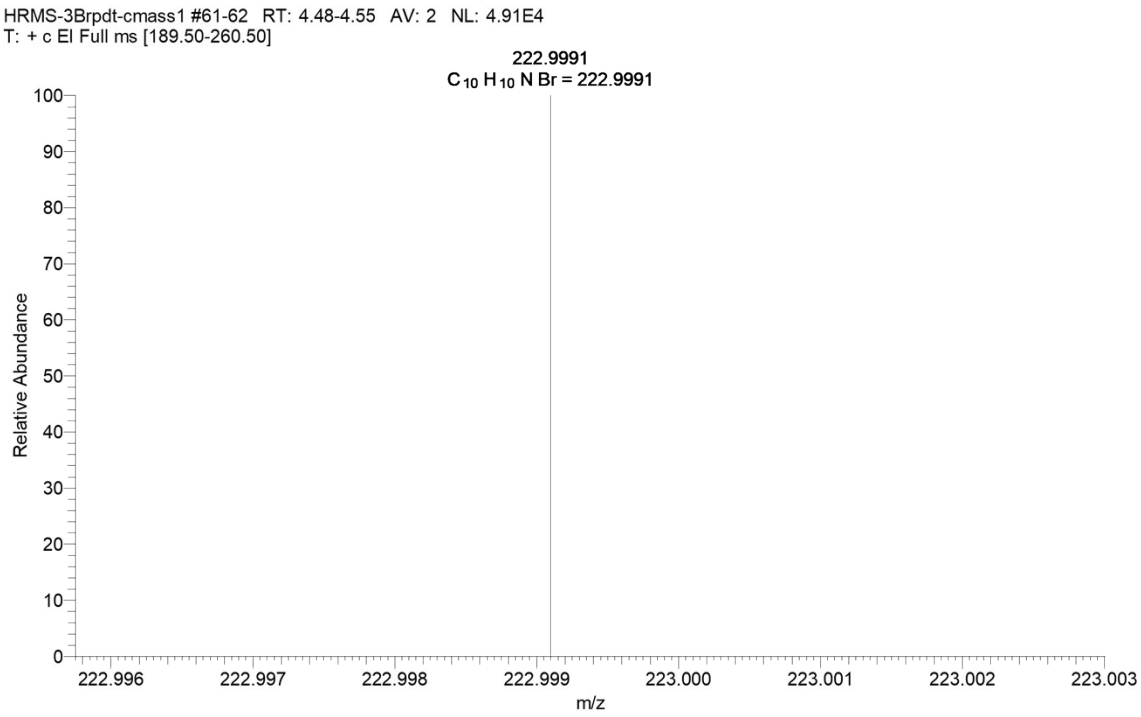

Figure S72. HRMS spectrum of **9l**.

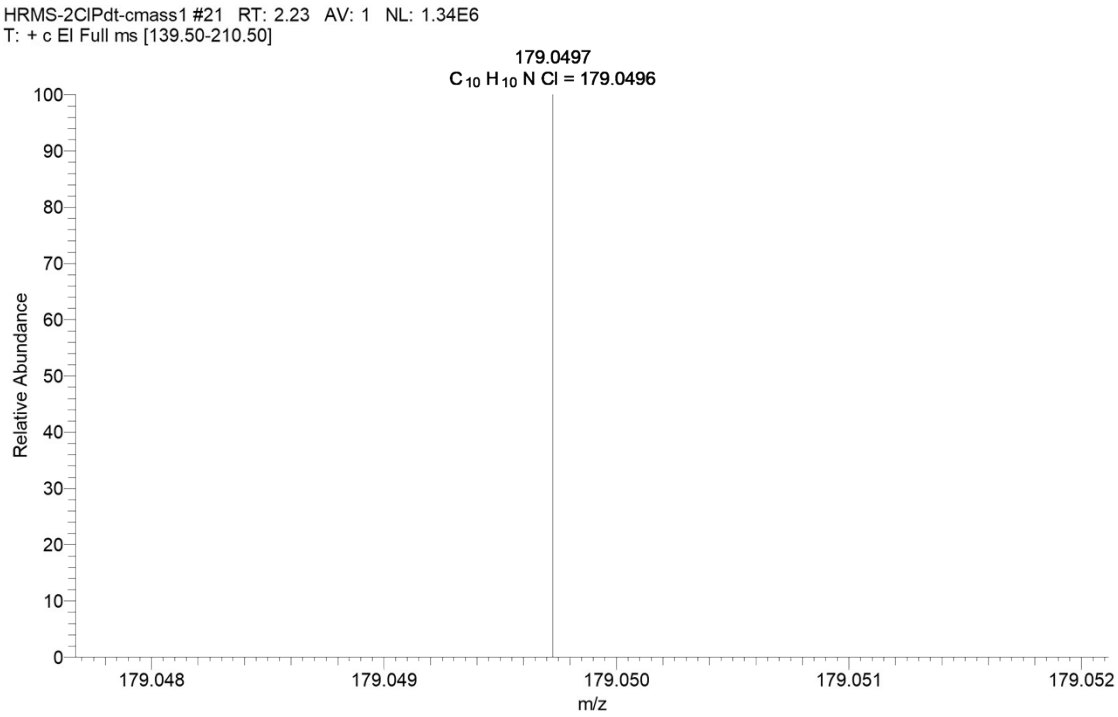

Figure S73. HRMS spectrum of **9m**.

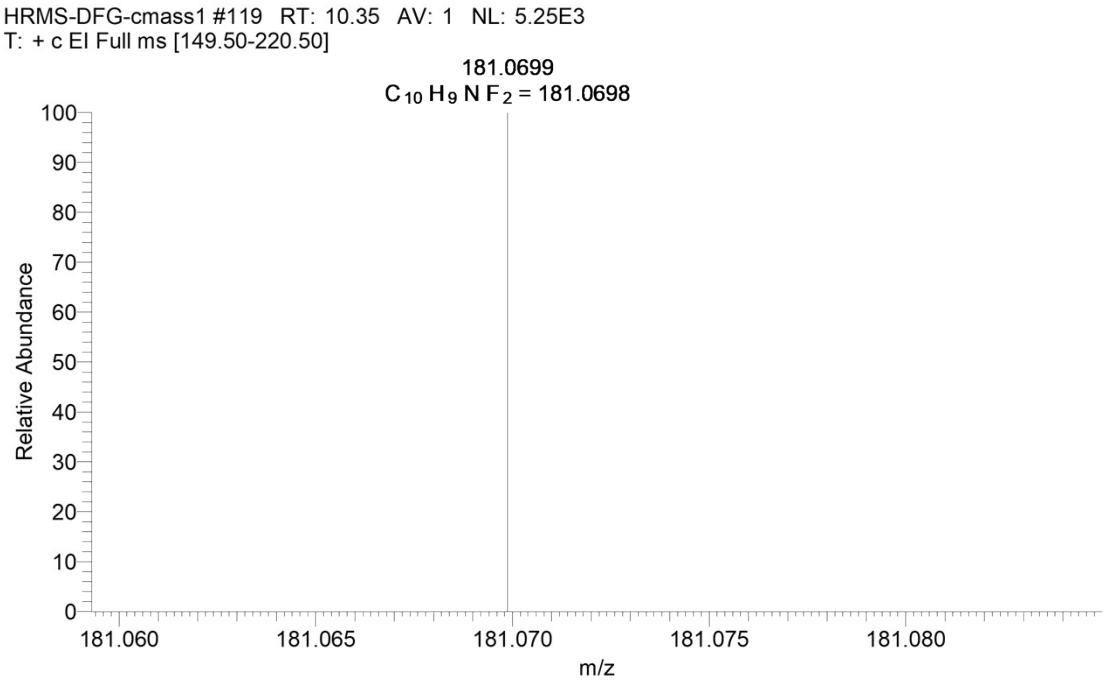

Figure S74. HRMS spectrum of **9o**.

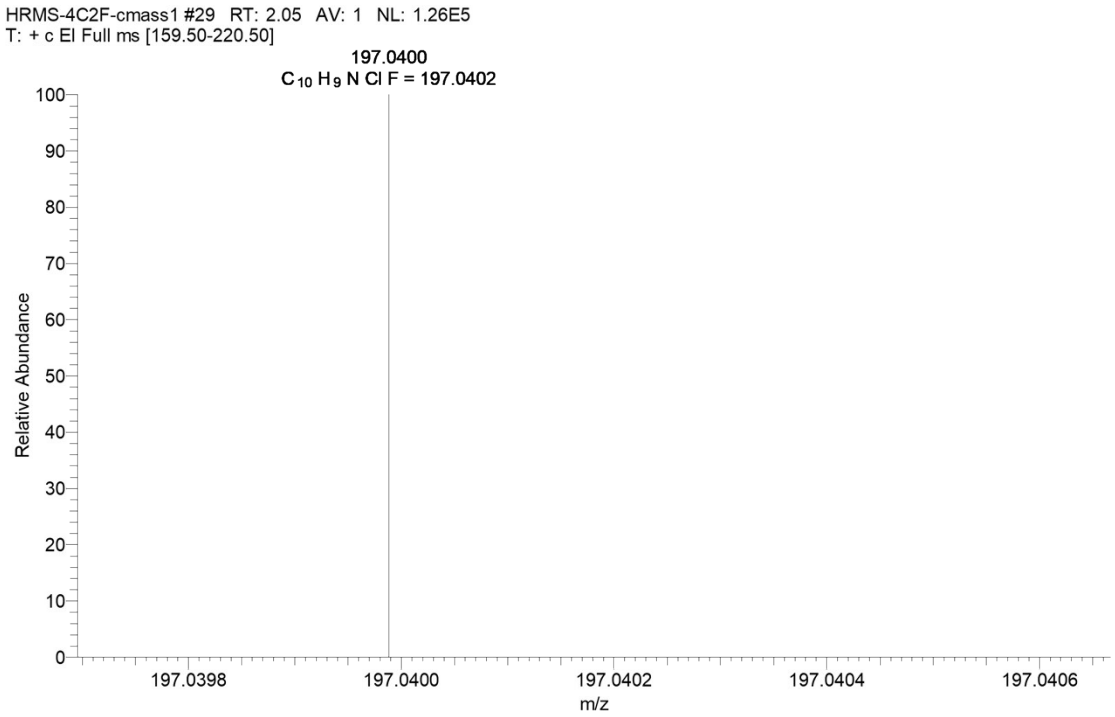

Figure S70. HRMS spectrum of **9q**.

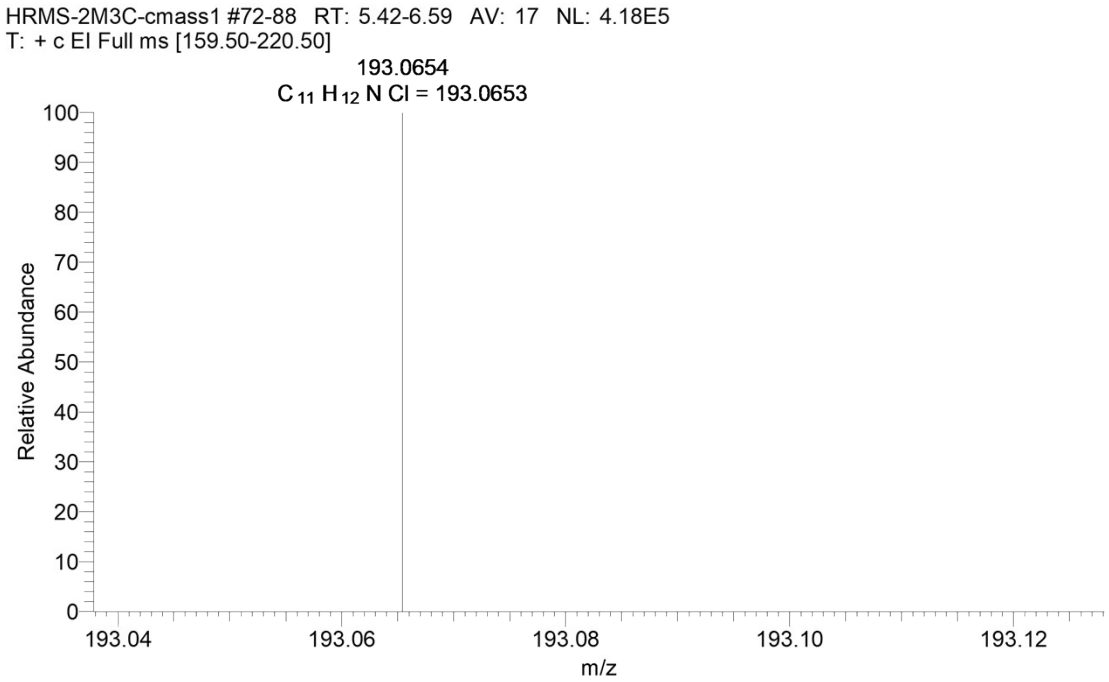

Figure S71. HRMS spectrum of **9r**.

Single Crystal X-ray diffraction study of the Ru complexes 7a, 7b & 7c

Single crystals of **7a, 7b & 7c** were grown by solvent diffusion method. The single crystal data collection of **7a** and **7c** were made on Bruker X8 prospector diffractometer by Cu-Kα. The reflection frames were then integrated with the Bruker SAINT Software package using a narrow-frame algorithm; the structures were solved using the Bruker SHELXTL Software Package. The single crystal data collection of **7b** was made on Rigaku Rapid II diffractometer by Mo-Kα This structure was then solved by 'crystalstructure' software package. Finally, all structures were refined using SHELXL-2017/1. All non-hydrogen atoms were refined anisotropically and hydrogen atoms were refined using the riding model. The crystal structures (thermal ellipsoid representation) of **7a, 7b & 7c** are given in **Figure S72-S74** and their various crystallographic data including crystal nature, data collection strategy and refinement parameters are summarized in the **Table S1**.

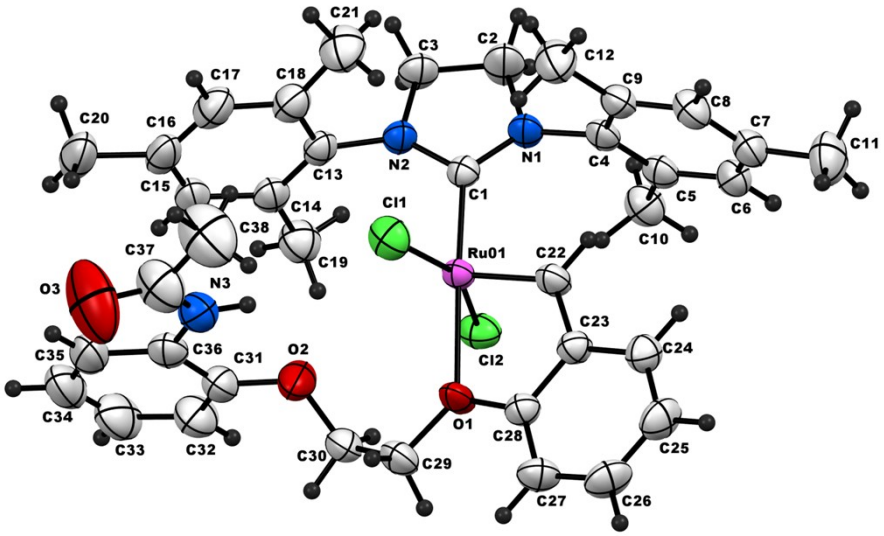

Figure S72. crystal structure (thermal ellipsoid representation; 50% probability) of **7a**.

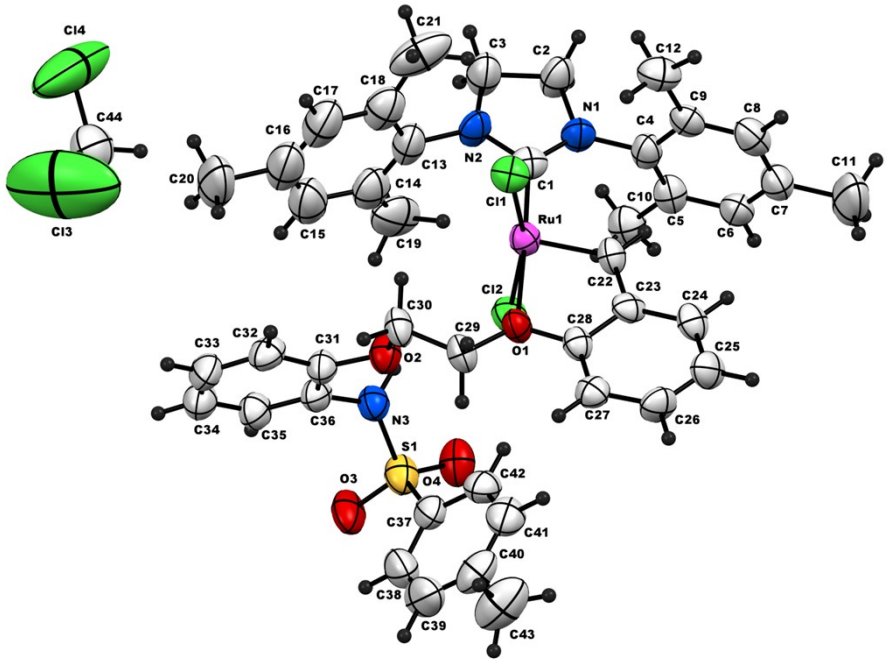

Figure S73. crystal structure (thermal ellipsoid representation; 50% probability) of **7b**.

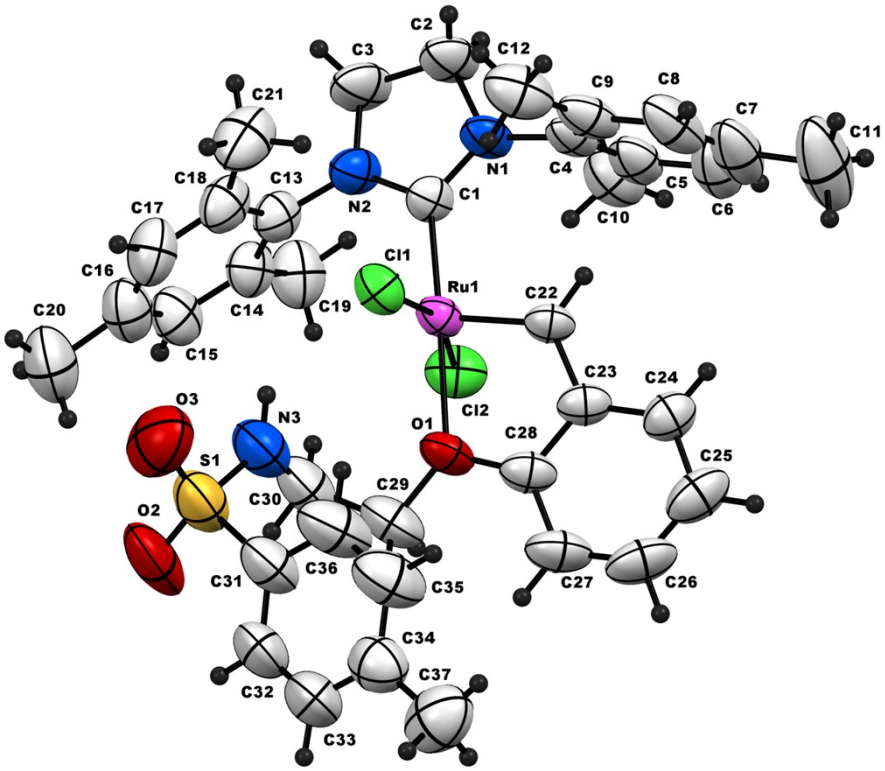

Figure S74. crystal structure (thermal ellipsoid representation; 50% probability) of **7c**.

Table S1. Summary on the nature and various crystallographic parameters of **7a, 7b & 7c**.

Crystal sample	**7a**	**7b**	**7c**
Chemical formula	$C_{38}H_{43}Cl_2N_3O_3Ru$	$C_{44}H_{49}Cl_4N_3O_4RuS$	$C_{37}H_{43}Cl_2N_3O_3RuS$
M_r	761.72	958.79	781.77
Crystal system, space group	Triclinic, *P*-1	Monoclinic, $P2_1/c$	Trigonal, *R* -3 :H
Temperature (K)	296	150	150
a, *b*, *c* (Å)	8.8611 (4), 10.6837 (5), 19.3949 (10)	12.038 (10), 14.886 (12), 24.180 (19)	28.6420 (5), 24.4463 (9)
α, β, γ (°)	74.511 (2), 87.898 (2), 89.558 (2)	90, 91.36 (3), 90	90, 90, 120
V (Å^3)	1768.22 (15)	4332 (6)	17368.0 (9)
Z	2	4	18
Radiation type	Cu *K*α	Mo *K*α	Cu *K*α
μ (mm^{-1})	5.30	0.70	5.36
Crystal size (mm)	0.21 × 0.20 × 0.08	0.10 × 0.05 × 0.04	0.18 × 0.14 × 0.12
Diffractometer	Bruker *APEX*-II CCD	Rigaku R-AXIS RAPID	Bruker *APEX*-II CCD
Absorption correction	Multi-scan	Multi-scan	Multi-scan
	SADABS2016/2 - Bruker AXS area detector scaling and absorption correction	*ABSCOR* (Rigaku, 1995)	*SADABS2016*/2 - Bruker AXS area detector scaling and absorption correction
T_{min}, T_{max}	0.220, 0.495	0.379, 0.972	0.45, 0.57
No. of measured, independent & observed [$I > 2\sigma(I)$] reflections	37958, 6204, 5934	24863, 7781, 3493	61572, 6025, 4870
R_{int}	0.040	0.171	0.067
$(\sin\theta/\lambda)_{max}$ (Å^{-1})	0.595	0.602	0.598
$R[F^2 > 2\sigma(F^2)]$, $wR(F^2)$, S	0.027, 0.069, 1.09	0.077, 0.214, 0.96	0.053, 0.151, 1.03
No. of reflections	6204	7781	6025
No. of parameters	431	515	431
H-atom treatment	Constrained	Constrained	Constrained
$\Delta\rho_{max}$, $\Delta\rho_{min}$ (e Å^{-3})	0.40, −0.29	1.01, −0.75	0.74, −0.51